Electronic Supporting Information for

Polyaminoborane main chain scission using N-heterocyclic carbenes; formation of donor-stabilised monomeric aminoboranes

Naomi E. Stubbs, Titel Jurca, Erin M. Leitao, Christopher H. Woodall and Ian Manners*

School of Chemistry, University of Bristol, Cantock's Close, Bristol BS8 1TS, UK

General Procedures, Reagents, and Equipment: All manipulations were carried out under an atmosphere of nitrogen gas using standard vacuum line and Schlenk techniques, or under an atmosphere of argon within an MBraun glovebox. All solvents were dried *via* a Grubbs design solvent purification system. Tri-cyclohexylphosphine (PCy_3), tri-*n*-butylphosphine ($P(nBu)_3$), 4-(Dimethylamino)pyridine (DMAP), diphenylamine (Ph_2NH) and tris(pentafluorophenyl)borane ($B(C_6F_5)_3$), were purchased from Sigma Aldrich Ltd. and purified by sublimation or distillation prior to use.

1,3-Bis(2,6-diisopropylphenyl)-1,3-dihydro-2*H*-imidazol-2-ylidene (IPr) and 1,3-Bis(2,4,6-trimethylphenyl)-1,3-dihydro-2*H*-imidazol-2-ylidene (IMes) were purchased from Sigma Aldrich Ltd. and used as acquired. Boron trichloride (1.0 M solution in hexanes) was purchased from Alfa Aesar and used as acquired.

Poly(ammonia-borane) ($[NH_2\text{-}BH_2]_n$), poly(methylaminoborane) ($[MeNH\text{-}BH_2]_n$), methylamine-borane ($MeNH_2\cdot BH_3$), diisopropylaminoborane ($iPr_2N{=}BH_2$) and cyclic tetramethyldiborazane ($[Me_2N\text{-}BH_2]_2$) were synthesized *via* literature methods[1,2] and purified by re-precipitation, distillation or sublimation prior to use as appropriate.

NMR spectra were recorded using Jeol ECP(Eclipse) 300 or Jeol ECP(Eclipse) 400 spectrometers. Chemical shifts are reported relative to external standards: $BF_3\cdot OEt_2$ (^{11}B). Integration of ^{11}B NMR spectra was performed using MestReNova Version 7.1.1-9649 with an estimated accuracy of ± 5%. Integrations are approximate and were rounded off to the nearest 10 %.

Electrospray ionisation (ESI) mass spectra were recorded using a cone potential of +150 V in a THF/acetonitrile mixture on a Bruker Daltonics Apex IV Fourier transform ion cyclotron mass spectrometer. Chemical ionisation (CI) mass spectra were obtained with the use of a VG Analytical Auto- Spec mass spectrometer employing chemical ionisation (CI) using a 70 eV electron impact ionisation source.

Gel permeation chromatography (GPC) samples were dissolved in the eluent (0.5 mg/mL) and filtered (Acrodisc, PTFE membrane, 0.45 mm) before analysis. GPC chromatography was performed on a Viscotek VE2001 instrument, using a flow rate of 1 mL/min of THF containing 0.1 w/w % nBu_4NBr, calibrated using polystyrene standards. The columns used were of grade GP5000HHR followed by GP2500HHR (Viscotek) at a constant temperature of 30 °C, and a VE 3580 refractometer was employed as the detector.

Elemental analysis was performed with a Eurovector EA 3000 Elemental Analyser at the University of Bristol Microanalysis Laboratory.

X-ray diffraction experiments on **1** were carried out at 100(2) K on a Bruker APEX II diffractometer using MoKα radiation (λ=0.71073Å). Data collection was performed using a CCD area detector from a single crystal mounted on a glass fiber. Intensities were integrated from several series of exposures. Absorption corrections were based on equivalent reflections using SADABS or TWINABS. The structures were solved using SHELXS and refined against all F_o^2 data with hydrogen atoms attached to carbon atoms riding in calculated positions using SHELXL. Further details are provided in Table S2.

Synthetic Procedures:

Synthesis and characterisation of $[MeNH\text{-}BH_2]_n$: To a solution of $MeNH_2{\cdot}BH_3$ (1.0 g, 22 mmol) in THF (1.2 mL), was added $IrH_2(POCOP)$ (POCOP = κ^3-1,3-$(OP\mathit{t}Bu_2)_2C_6H_3$) (40 mg, 0.07 mmol, 0.3 mol%) in THF (0.8 mL) at 0 °C. The mixture was allowed to stir at 20 °C for 1 h, where the reaction was tracked by ^{11}B NMR and it was observed that complete conversion to $[MeNH\text{-}BH_2]_n$ occurred. This is the method reported in literature.[1] The product was purified by re-precipitation from minimal THF (*ca.* 1 mL) and hexanes (*ca.* 200 mL) three times. Yield: 0.6 g (60 %), ^{11}B NMR (96 MHZ, THF) δ -7.6 ppm (br) (Fig. S1); ESI-MS (See Fig. S2); GPC: M_n = 190 000 Da, PDI = 1.21 (Fig. S3).

Thermal reaction of $[MeNH\text{-}BH_2]_n$ in THF: To solid $[MeNH\text{-}BH_2]_n$ (27 mg, 0.63 mmol), THF (1 mL) was added at 20 °C. The mixture was heated to 70 °C for 19 h in a closed system. Analysis of the reaction solution by ^{11}B NMR revealed partial depolymerisation to lower molecular weight polymer $[MeNH\text{-}BH_2]_x$ (δ(^{11}B) -6.6 ppm, br) (*ca.* 90 %), as indicated by a sharpening of the peak as well as the presence of $[MeN\text{-}BH]_3$ (δ(^{11}B) 32.3 ppm, d, $^1J_{BH}$ = 135 Hz) (*ca.* 10 %) (Fig. S4). ESI-MS analysis on the reaction solution confirmed the presence of oligo(aminoborane) with the observation of peaks with *m/z* difference of 43 (Fig. S5). Isolation of the material was achieved by the solvent and volatile products being removed under vacuum, and analysis by GPC (M_n = 66 000 Da, PDI = 2.03) (Fig. S6) confirmed the presence of polymeric material.

Thermal reaction of $[MeNH\text{-}BH_2]_n$ in toluene: To solid $[MeNH\text{-}BH_2]_n$ (27 mg, 0.63 mmol), toluene (1 mL) was added at 20 °C. The mixture was heated to 70 °C for 19 h in a closed system. Analysis of the reaction solution by ^{11}B NMR revealed partial depolymerisation to $[MeNH\text{-}BH_2]_x$ (δ(^{11}B) -5.3 ppm, br) (*ca.* 80 %), as indicated by a sharpening of the peak, as well as the presence of $[MeN\text{-}BH]_3$ (δ(^{11}B) 32.9 ppm, d, $^1J_{BH}$ = 137 Hz) (*ca.* 10 %), $MeNH_2{\cdot}BH_3$ (δ(^{11}B) -18.7 ppm, q, $^1J_{BH}$ = 95 Hz) (*ca.* 10 %) and $BH_2(\mu\text{-}MeNH)(\mu\text{-}H)BH_2$ (δ(^{11}B) -23.0 ppm, br) (trace amounts) (Fig. S7). ESI-MS analysis on the reaction solution confirmed the presence of oligo(aminoborane) with the observation of peaks with *m/z* difference of 43 (Fig. S8). Isolation of the material was achieved by the solvent and volatile products being removed under vacuum, and analysis by GPC (M_n = 65 000 Da, PDI = 2.07 (Fig. S9) confirmed the presence of polymeric material.

Reaction of $[MeNH\text{-}BH_2]_n$ with PCy_3: To solid $[MeNH\text{-}BH_2]_n$ (50 mg, 1.16 mmol), a solution of PCy_3 (325 mg, 1.16 mmol) in toluene (3 mL) was added at 20 °C. The mixture was heated at 50 °C for 22 h, and monitored by ^{11}B NMR spectroscopy, which revealed no obvious change with the observation of high molecular weight $[MeNH\text{-}BH_2]_n$ ($\delta(^{11}B)$ -9.3 ppm, br) (Fig. S10).

Reaction of $[MeNH\text{-}BH_2]_n$ with $P(nBu)_3$: To solid $[MeNH\text{-}BH_2]_n$ (50 mg, 1.16 mmol), a solution of $P(nBu)_3$ (0.3 mL, 1.16 mmol) in THF (2 mL) was added at 0 °C. The mixture was allowed to stir at 20 °C for 22 h and monitored by ^{11}B and ^{31}P NMR spectroscopy, which revealed partial depolymerisation to $[MeNH\text{-}BH_2]_{3 or x}$ ($\delta(^{11}B)$ -5.8 ppm, br) (*ca.* 60 %), as indicated by the sharpening of the peak, and decomposition to $(MeNH)_2BH$ ($\delta(^{11}B)$ 27.8 ppm, d, br) (trace amounts), an unassigned product ($\delta(^{11}B)$ 0.8 ppm, s) (*ca.* 30 %) and $MeNH_2\cdot BH_3$ ($\delta(^{11}B)$ -18.8 ppm, q, $^1J_{BH}$ = 89 Hz) (*ca.* 10%) (Fig. S11) with negligible change to $P(nBu)_3$ ($\delta(^{31}P)$ -31.4 ppm, s) (Fig. S12).

Reaction of $[MeNH\text{-}BH_2]_n$ with 4-dimethylaminopyridine (DMAP): To solid $[MeNH\text{-}BH_2]_n$ (25 mg, 0.58 mmol), a solution of DMAP (65 mg, 0.58 mmol) in THF (1.5 mL) was added at 20 °C. The mixture was allowed to stir at 20 °C for 24 h and monitored by ^{11}B NMR spectroscopy, which revealed depolymerisation to $[MeNH\text{-}BH_2]_{3 or x}$ ($\delta(^{11}B)$ -5.3 ppm, br) (*ca.* 70 %), as indicated by a sharpening of the peak, as well as decomposition to $[MeN\text{-}BH]_3$ ($\delta(^{11}B)$ 30.2 ppm, d, br) (*ca.* 10 %), $(MeNH)_2BH$ ($\delta(^{11}B)$ 27.7 ppm, d, br) (trace amounts), $BH_3\cdot THF$ ($\delta(^{11}B)$ 1.7 ppm, q, br) (trace amounts) and $MeNH_2\cdot BH_3$ ($\delta(^{11}B)$ -18.9 ppm, $^1J_{BH}$ = 97 Hz) (*ca.* 10 %) (Fig. S13).

Synthesis of $MeNH\text{-}BH_2\text{-}IPr$: To solid $[MeNH\text{-}BH_2]_n$ (11 mg, 0.26 mmol), a solution of IPr (100 mg, 0.26 mmol) in THF (0.7 mL) was added at 20 °C. After stirring at 20 °C, the mixture was tracked by ^{11}B NMR spectroscopy at 10 min and 1 h which revealed quantitative formation of $MeNH\text{-}BH_2$-IPr. The solvent was removed under vacuum along with any volatiles with the remaining solid re-dissolved in C_6D_6 to obtain ^{11}B, ^{1}H and ^{13}C NMR spectra. Attempts to isolate $MeNH\text{-}BH_2$-IPr by re-precipitation were conducted by dissolving solid $[MeNH\text{-}BH_2]_n$ (8 mg, 0.19 mmol) and solid IPr (75 mg, 0.19 mmol) in minimal DCM (0.3 mL) and the solution was transferred into hexanes (1.5 mL) to precipitate out a colourless solid. After centrifuging the solid for 1 min at 60,000 rpm, the solvent was decanted off with the remaining colourless solid dried under vacuum with a mass of 37 mg. Analysis of the isolated product revealed no signal by ^{11}B NMR with analysis by ^{1}H NMR indicating the presence of IPr (Fig. S19), suggesting that cleavage between $[MeNH\text{-}BH_2]$ and IPr occurred. ^{11}B NMR (96 MHz, THF) δ -17.2 ppm (t, $^1J_{BH}$ = 90 Hz) (Fig. S14). ^{11}B NMR (96 MHz, MHz, C_6D_6): δ -16.2 ppm (t, $^1J_{BH}$ = 90 Hz) (Fig. S15). ^{1}H NMR (400 MHz, C_6D_6): δ 7.25-7.09 ppm (m, 6H, Ar*H*), 6.32 ppm (s, 2H, N-C*H*-), 2.78 ppm (m, 4H, $(CH_3)_2$-C*H*-), 2.49 ppm (s, 3H, N-C*H*$_3$), 1.41 ppm (d, $^3J_{HH}$ = 6.8 Hz, 12H, $(CH_3)_2$-CH-), 1.06 ppm (d, $^3J_{HH}$ = 7.0 Hz, 12H, $(CH_3)_2$-CH-) (Fig. S16). ^{13}C NMR (101 MHz, C_6D_6): δ 145.4 ppm (Ar*C*), 134.6 ppm (Ar*C*), 129.9 ppm (Ar*C*), 123.6 ppm (Ar*C*), 121.5 ppm (-N-*C*H), 38.6 ppm (N-*C*H$_3$), 28.5 ppm (*i*Pr), 24.7 ppm (*i*Pr), 22.8 ppm (*i*Pr) (Fig. S17). MS (ESI): *m/z*: 389 [M^+-NMeH-BH_2] (100 %), 432 [M^+] (35 %) (Fig. S18).

Synthesis of $MeNH\text{-}BH_2\text{-}IMes$: To solid $[MeNH\text{-}BH_2]_n$ (10.3 mg, 0.24 mmol), a solution of IMes (75 mg, 0.24 mmol) in THF (0.7 mL) was added at 20 °C. After stirring at 20 °C for 10 min, the mixture was analysed by ^{11}B NMR spectroscopy, which revealed *ca.* 60 % formation of $MeNH\text{-}BH_2$-IMes and peaks corresponding to $[MeNH\text{-}BH_2]_3$, ($\delta(^{11}B)$ -5.5 ppm, t, br) (*ca.* 20 %) as well as unassignable products (δ(^{11}B) 1.1 ppm, br) (*ca.* 10 %) and (δ(^{11}B) -1.9 ppm, s) (trace amounts). ^{11}B NMR (96 MHz, THF) δ -17.0 ppm (t, $^{1}J_{BH}$ = 90 Hz) (*ca.* 60 %) (Fig. S20). MS (ESI): *m/z*: 305 [M^+-MeNH-BH_2] (100 %), 348 [M^+] (5 %) (Fig. S21).

Synthesis of NH_2-BH_2-IPr: To insoluble solid [NH_2-BH_2]$_n$ (8 mg, 0.26 mmol), a solution of IPr (100 mg, 0.26 mmol) in THF (1 mL) was added at 20 °C. After stirring at 20 °C for 24 h, the mixture was analysed by ^{11}B NMR spectroscopy which revealed *ca.* 90 % formation of NH_2-BH_2-IPr and a peak corresponding to an unassignable product (δ(^{11}B) -1.8 ppm, s) (trace amounts). ^{11}B NMR (96 MHz, THF) δ -19.5 ppm (t, $^{1}J_{BH}$ = 88 Hz) (*ca.* 90 %) (Fig. S22). MS (CI): *m/z*: 389 [M^+-NH_2-BH_2] (100 %), 417 [M^+] (24 %) (Fig. S23).

Synthesis of *i*Pr_2N-BH_2-IPr: To a solution of *i*Pr_2N=BH_2 in THF (0.45 mL, 0.29 M, 0.13 mmol), a solution of IPr (50 mg, 0.13 mmol) in THF (0.25 mL) was added at 20 °C. After stirring at 20 °C for 2 h, the mixture was analysed by ^{11}B NMR spectroscopy which revealed quantitative formation of *i*Pr_2N-BH_2-IPr. The solvent was removed under vacuum along with any volatiles, with the remaining solid re-dissolved in C_6D_6 to obtain ^{11}B, ^{1}H and ^{13}C NMR spectra. Attempts to isolate product by re-precipitation were conducted by dissolving liquid *i*Pr_2N=BH_2 (22 mg, 0.19 mmol) and solid IPr (75 mg, 0.19 mmol) in minimal DCM (0.3 mL) and the solution transferred into hexanes (1.5 mL) to precipitate out a colourless solid. After centrifuging the solid for 1 min at 60,000 rpm, the solvent was decanted off and the remaining colourless solid was dried under vacuum, yielding a mass of 7 mg. Analysis of the isolated product revealed no signal by ^{11}B NMR, with analysis by ^{1}H NMR indicating the presence of IPr (Fig. S29), suggesting that cleavage between [*i*Pr_2N-BH_2] and IPr occurred. ^{11}B NMR (96 MHz, THF) δ -19.8 ppm (br) (Fig. S24). ^{11}B NMR (96 MHz, C_6D_6) δ -19.0 ppm (br) (Fig. S25). ^{1}H NMR (400 MHz, C_6D_6) δ 7.20-7.08 ppm (m, 6H, Ar*H*), 6.44 ppm (s, 2H, N-C*H*-), 2.83 ppm (m, 6H, C*H*-CH_3), 1.29 ppm (d, $^{3}J_{HH}$ = 6.8 Hz, 12H, C-CH-CH_3), 1.04 ppm (d, $^{3}J_{HH}$ = 6.9 Hz, 12 H, C-CH-CH_3), 0.95 ppm (d, $^{3}J_{HH}$ = 6.5 Hz, 12H, N-CH-CH_3) (Fig. S26). ^{13}C NMR (101 MHz, C_6D_6) δ 147.5 ppm (Ar*C*), 129.2 ppm (Ar*C*), 123.5 ppm (Ar*C*), 121.7 ppm (N-*C*H), 49.2 ppm (N-*i*Pr), 28.6 ppm (C-*i*Pr), 24.5 ppm (C-*i*Pr), 23.5 ppm (C-*i*Pr), 22.8 ppm (C-*i*Pr) (Fig. S27). MS (ESI): *m/z*: 389 [M^+-N*i*Pr_2-BH_2] (100 %), 502 [M^+] (56 %) (Fig. S28).

Synthesis of Me_2N-BH_2-IPr: To solid [Me_2N-BH_2]$_2$ (12 mg, 0.10 mmol), a solution of IPr (75 mg, 0.19 mmol) in THF (0.7 mL) was added at 20 °C. After stirring at 60 °C for 24 h, the mixture was analysed by ^{11}B NMR spectroscopy, which revealed near quantitative conversion to Me_2N-BH_2-IPr and a peak corresponding to an unassignable product (δ(^{11}B) -1.7 ppm, s) (trace amounts). ^{11}B NMR (96 MHz, THF) δ -14.1 ppm (t, $^{1}J_{BH}$ = 89 Hz) (Fig. S30). MS (ESI): *m/z*: 389 [M^+-BH_2-NMe_2] (100 %), 446 [M^+] (8 %) (Fig. S31).

Reaction of $MeNH_2{\cdot}BH_3$ with two equivalents of IPr: To solid $MeNH_2{\cdot}BH_3$ (5 mg, 0.10 mmol), a solution of IPr (78 mg, 0.20 mmol) in THF (1 mL) was added at 20 °C. The mixture was allowed to stir at 20 °C for 24 h and monitored by ^{11}B NMR spectroscopy, which revealed *ca.* 80 % conversion to MeNH-BH_2-IPr and peaks corresponding to an unassignable product (δ(^{11}B) 28.5 ppm, br) (*ca.* 10

%) and $MeNH_2{\cdot}BH_3$ (δ(^{11}B) -19.4 ppm, t, br) (trace amounts). ^{11}B NMR (96 MHz, THF) δ -16.5 ppm (t, $^{1}J_{BH}$ = 88 Hz) (*ca.* 80 %) (Fig. S32).

Reaction of $MeNH_2{\cdot}BH_3$ with three equivalents of IPr: To solid $MeNH_2{\cdot}BH_3$ (5 mg, 0.11 mmol), a solution of IPr (129 mg, 0.33 mmol) in THF (1 mL) was added at 20 °C. The mixture was allowed to stir at 20 °C for 8 h and monitored by ^{11}B NMR spectroscopy, which revealed *ca.* 90 % conversion to MeNH-BH_2-IPr and peaks corresponding to unassignable products (δ(^{11}B) 28.8 ppm (br) (trace amounts) and (δ(^{11}B) -1.78 ppm (s) (trace amounts). ^{11}B NMR (96 MHz, THF) -16.5 ppm (t, $^{1}J_{BH}$ = 90 Hz) (*ca.* 90 %) (Fig. S33).

Synthesis of $Ph_2N{=}BCl_2$: To a solution of Ph_2NH (5 g, 0.03 mol) in Et_2O (100 mL) was added dropwise, a solution of *n*BuLi in hexanes (18.5 mL, 1.6 M, 0.03 mol) at -78 °C. The mixture was allowed to warm to 20 °C for 1 h before a solution of BCl_3 in hexanes (30 mL, 1.0 M, 0.03 mol) was added dropwise at -78 °C. After 30 min at -78 °C, the mixture was allowed to warm to 20 °C and stirred for 2 h. Solid by-product LiCl was removed by canula filtration and solvent was removed under vacuum. The product was isolated by precipitation from a solution of hexanes at -10 °C to yield a colourless solid. The liquid was decanted off and the remaining colourless solid was dried under vacuum. Yield: 2.5 g (33 %). ^{11}B NMR (96 MHz, C_6D_6) δ 31.6 ppm (s) (Fig. S34). ^{1}H (400 MHz, C_6D_6) δ 6.98-6.85 ppm (m, 10H, Ar*H*) (Fig. S35). ^{13}C NMR (101 MHz, C_6D_6) δ 146.1 ppm (*i*-Ar-*C*), δ 129.0 ppm (*o*/*m*-Ar-*C*), δ 127.4 ppm (*o*/*m*-Ar-*C*), δ 126.5 ppm (*p*-Ar-*C*) (Fig. S36). Elemental analysis calcd (%) for $C_{12}H_{10}BNCl_2$: C 57.67, H 4.03, N 5.60; found: C 57.98, H 4.32, N 5.45.

Synthesis of Ph_2N-BCl_2-IPr (1): To solid $Ph_2N{=}BCl_2$ (128 mg, 0.51 mmol), a solution of IPr (200 mg, 0.51 mmol) in THF (1 mL) was added at 20 °C. The mixture was allowed to stir at 20 °C for 1 h and monitored by ^{11}B NMR spectroscopy that revealed complete conversion to Ph_2N-BCl_2-IPr. To obtain isolated product, to solid $Ph_2N{=}BCl_2$ (128 mg, 0.51 mmol), a solution of IPr (200 mg, 0.51 mmol) in minimal THF (0.5 mL) was added at 20 °C. After stirring at 20 °C for 1 h, the solution was transferred into hexanes (5 mL) to precipitate out a colourless solid. The liquid was decanted off and remaining colourless solid dried under vacuum. Crystals suitable for single-crystal X-ray diffraction were obtained from a saturated toluene solution of **1** over several days at 20 °C (For crystal structure, see Fig. 1 and S42). Yield: 120 mg (37 %) ^{11}B NMR (96 MHz, THF) δ 1.2 ppm (s) (Fig, S37). ^{11}B NMR (96 MHz, C_6D_6) δ 1.2 ppm (s) (Fig. S38). ^{1}H NMR (96 MHz, C_6D_6) δ 7.25 ppm (t, 2H, C-N-*p*-Ar-H), δ 7.12-7.07 ppm (m, 8H, B-N-*o*/*m*-Ar-*H*), δ 6.85 ppm (t, 2H, B-N-*p*-Ar*H*), δ 6.58 ppm (br, 4H, C-N-*m*-Ar-*H*), δ 6.41 ppm (s, 2H, N-C*H*), δ 2.99 ppm (m, 4H, $(CH_3)_2$-C*H*), δ 1.22 ppm (br, 12H, $(CH_3)_2$-CH), δ 0.93 ppm (d, 12H, $(CH_3)_2$-CH) (Fig. S39). ^{13}C NMR (101 MHz, C_6D_6) δ 135.7 ppm (Ar*C*), 130.5 ppm (Ar*C*), 124.7 ppm (Ar*C*), 124.2 ppm (N-*C*H), 29.4 ppm (*i*Pr), 26.1 ppm (*i*Pr), 22.2 ppm (*i*Pr) (Fig. S40).

Regeneration of *i*Pr_2N-BH_2-IPr with $B(C_6F_5)_3$ in toluene: To a solution of *i*$Pr_2N{=}BH_2$ (29 mg, 0.26 mmol) in toluene (0.7 mL), a solution of IPr (100 mg, 0.26 mmol) in toluene (0.8 mL) was added at 20 °C. After 10 min once *i*Pr_2N-BH_2-IPr (δ(^{11}B) -17.3 ppm, br) had formed, a solution of $B(C_6F_5)_3$ (132 mg, 0.26 mmol) in toluene (0.3 mL) was added at 20 °C and tracking by ^{11}B NMR after 1 h revealed presence of *i*$Pr_2N{=}BH_2$ (δ(^{11}B) 34.6 ppm, t, $^1J_{BH}$ = 128 Hz) (*ca.* 40 %) and IPr·$B(C_6F_5)_3$ (δ(^{11}B) -16.2 ppm, s) (*ca.* 60 %) as well as an unassignable product (δ(^{11}B) -14.4 ppm, s) (trace amounts) (Fig. S41). Two more subsequent addition of solutions of IPr (100 mg, 0.26 mmol) and $B(C_6F_5)_3$ (132 mg, 0.26 mmol) in toluene (0.3 mL) were added at 20 °C (Fig. 2).

Spectroscopic data:

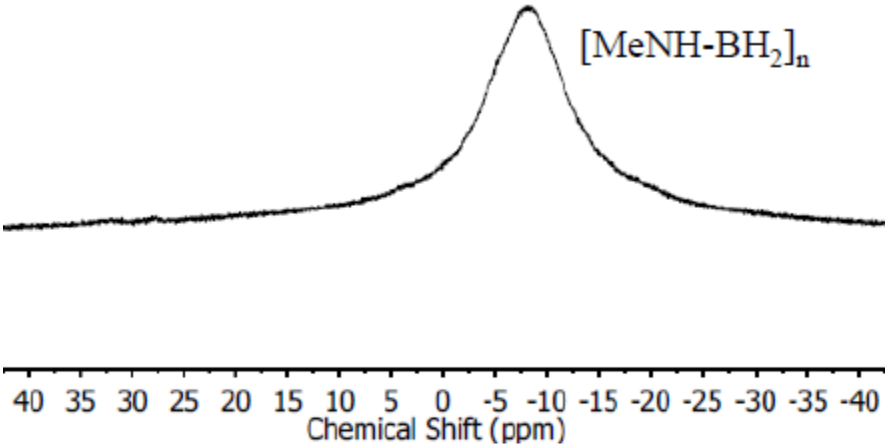

Figure S1: ^{11}B {^{1}H} NMR of isolated $[MeNH\text{-}BH_2]_n$ in $CDCl_3$ produced from $MeNH_2{\cdot}BH_3$ and 0.3 mol% IrH_2(POCOP) in THF at 20 °C.

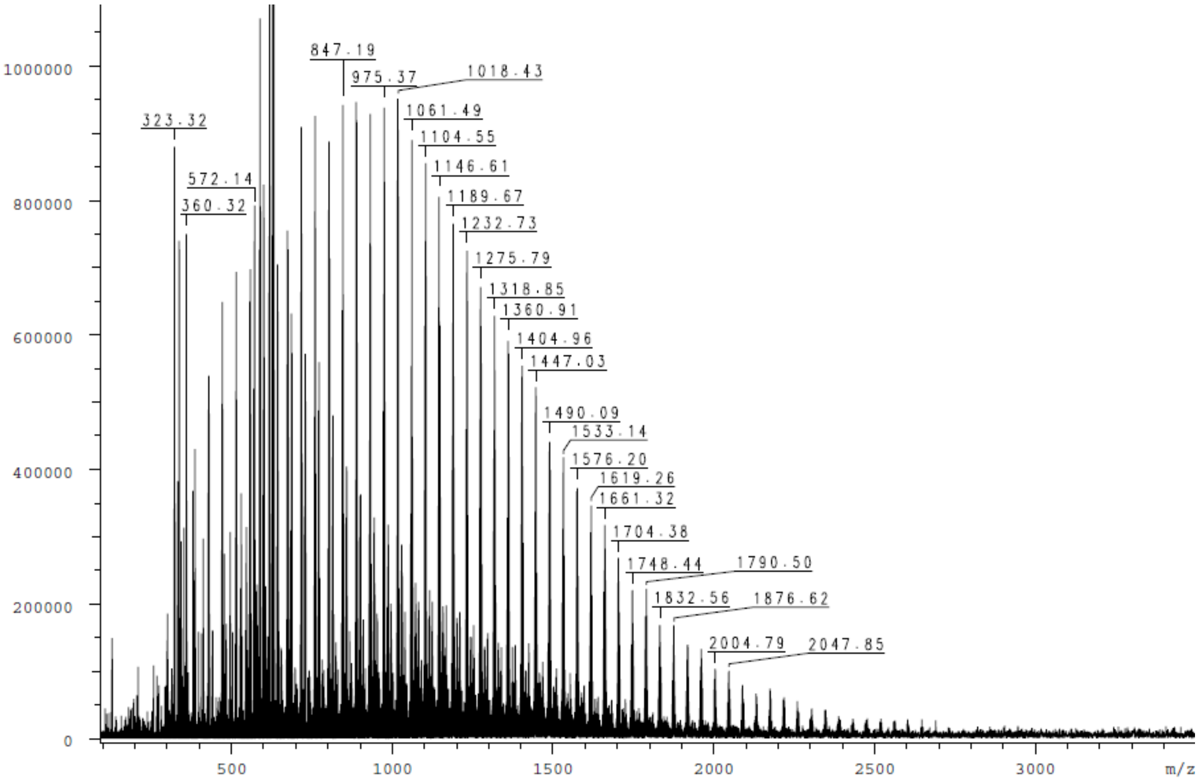

Figure S2(a): ESI-MS spectrum of isolated $[MeNH\text{-}BH_2]_n$ produced from $MeNH_2{\cdot}BH_3$ and 0.3 mol% IrH_2(POCOP) in THF at 20 °C. Repeat unit: 43 *m/z*.

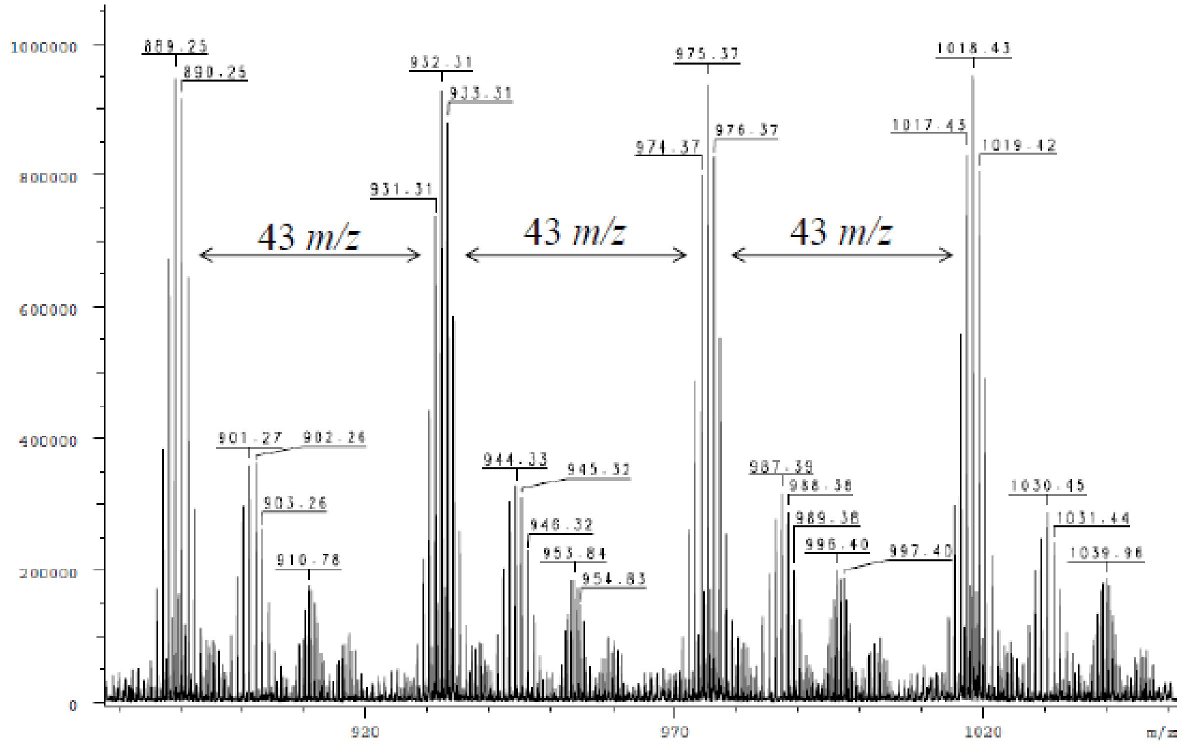

Figure S2(b): Enlarged view of a section of the ESI-MS spectrum of isolated $[MeNH\text{-}BH_2]_n$ produced from $MeNH_2{\cdot}BH_3$ and 0.3 mol% IrH_2(POCOP) in THF at 20 °C. Repeat unit: 43 *m/z*.

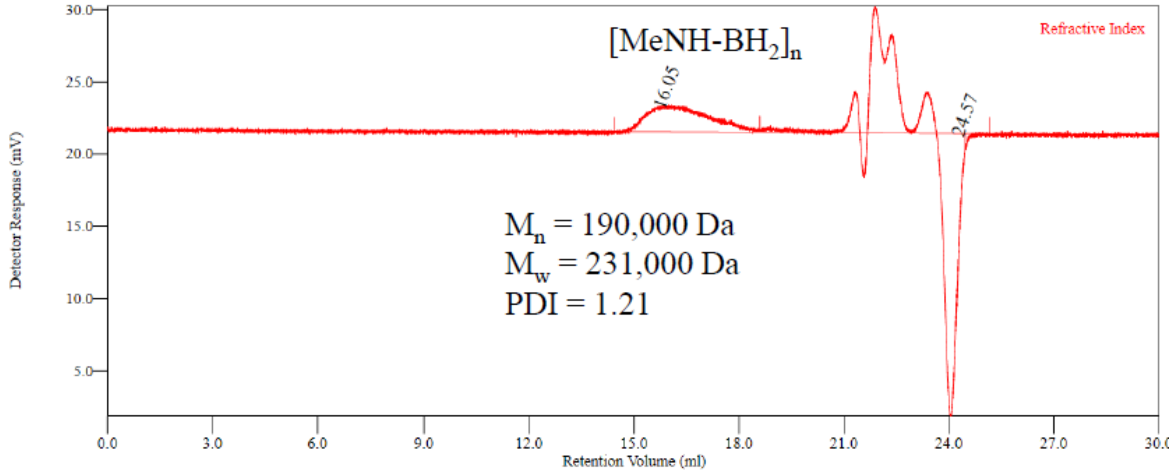

Figure S3: GPC trace of isolated $[MeNH\text{-}BH_2]_n$ produced from $MeNH_2{\cdot}BH_3$ and 0.3 mol% IrH_2(POCOP) in THF at 20 °C. The various peaks at 21 – 24 min are a result of the sample injection.

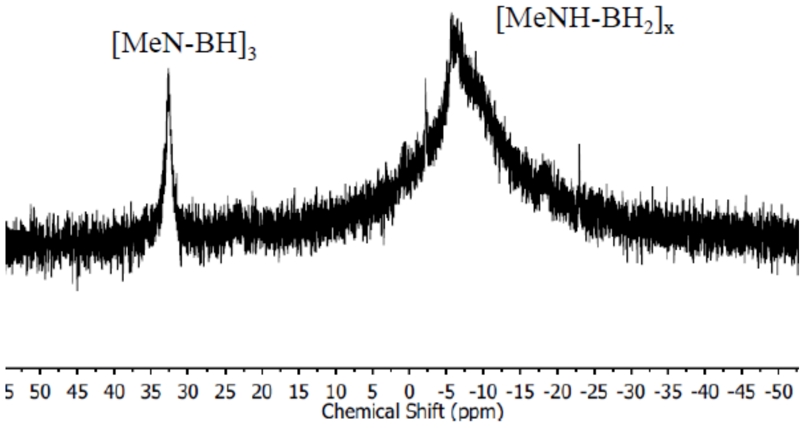

Figure S4(a): ^{11}B {^{1}H} NMR of reaction solution of [MeNH-BH$_2$]$_n$ after heating in THF at 70 °C for 19 h.

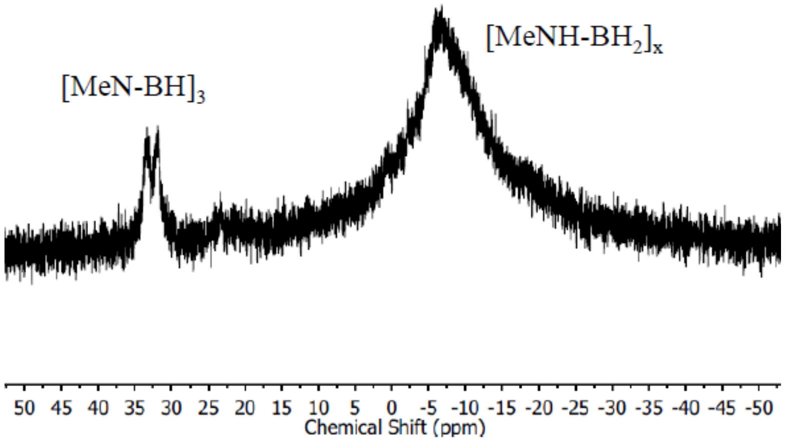

Figure S4(b): ^{11}B NMR of reaction solution of [MeNH-BH$_2$]$_n$ after heating in THF at 70 °C for 19 h.

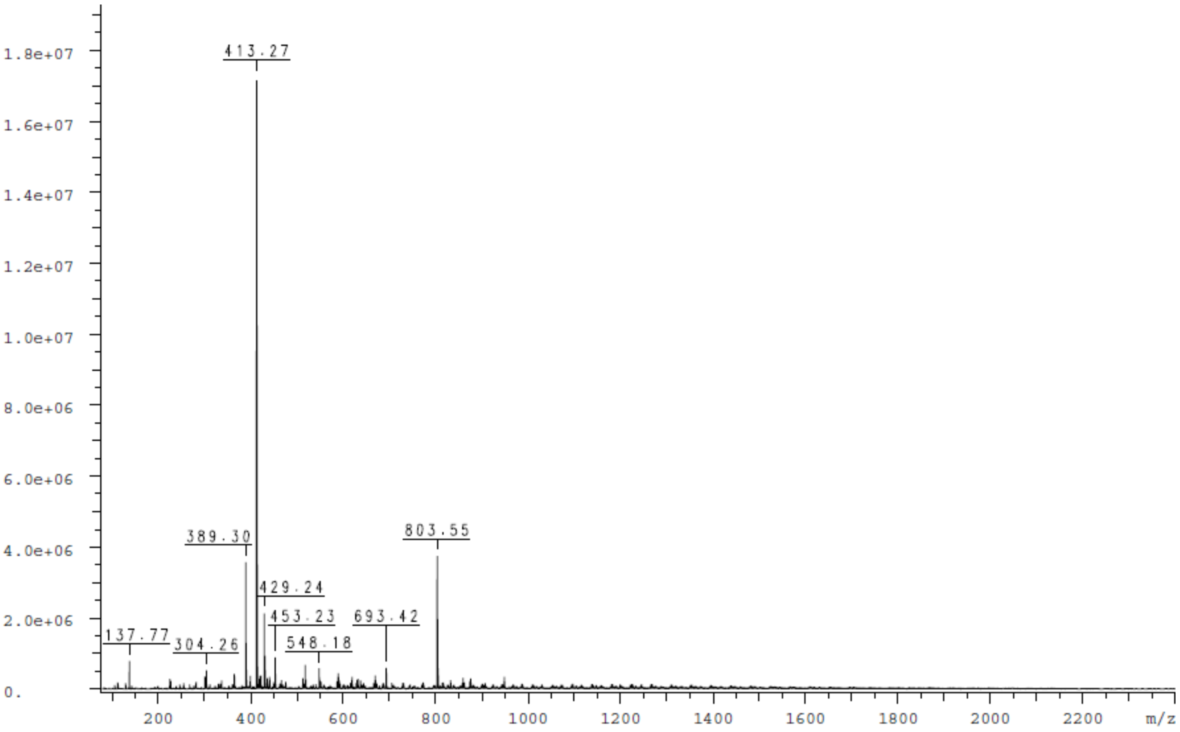

Figure S5(a): ESI-MS of the reaction solution of $[MeNH\text{-}BH_2]_n$ after heating in THF at 70 °C for 19 h.

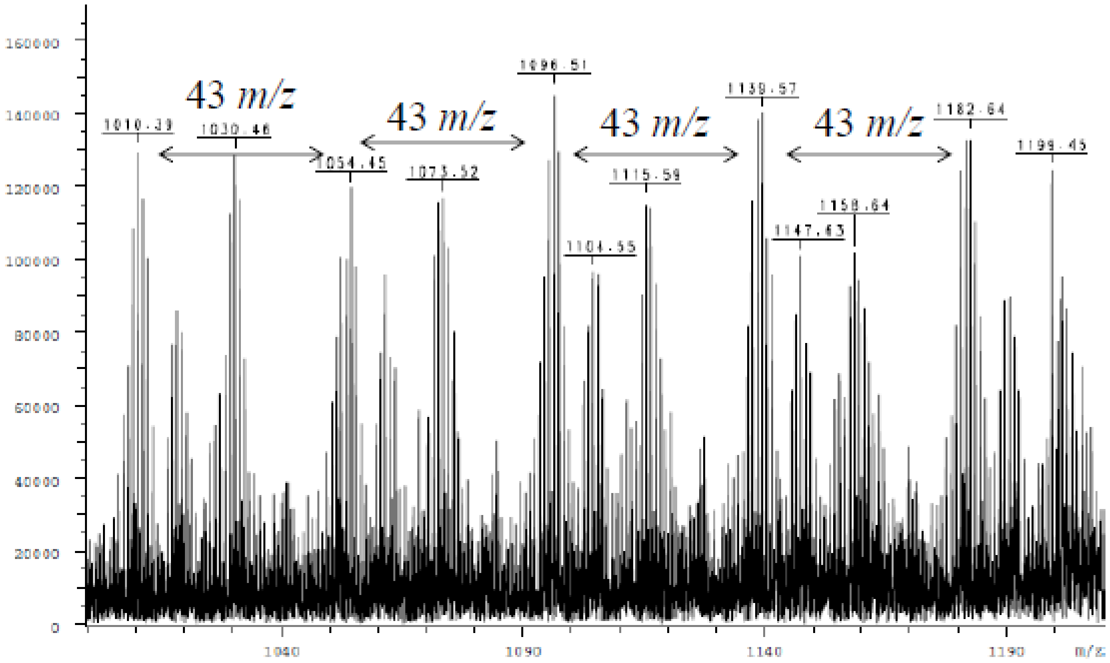

Figure S5(b): Enlarged view of a section of ESI-MS of the reaction solution of $[MeNH\text{-}BH_2]_n$ after heating in THF at 70 °C for 19 h.

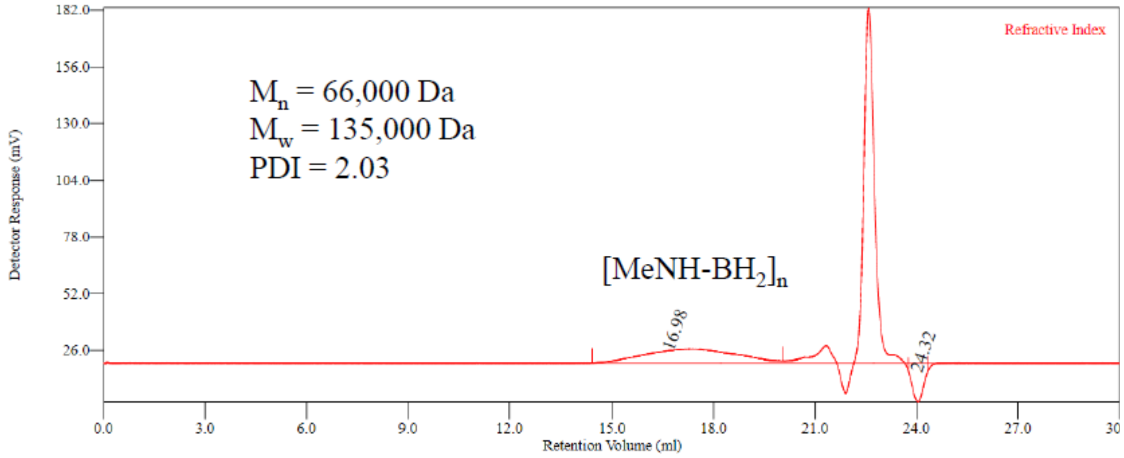

Figure S6: GPC trace of isolated [MeNH-BH$_2$]$_n$ after heating in THF at 70 °C for 19 h. The various peaks at 21 – 24 min are a result of the sample injection.

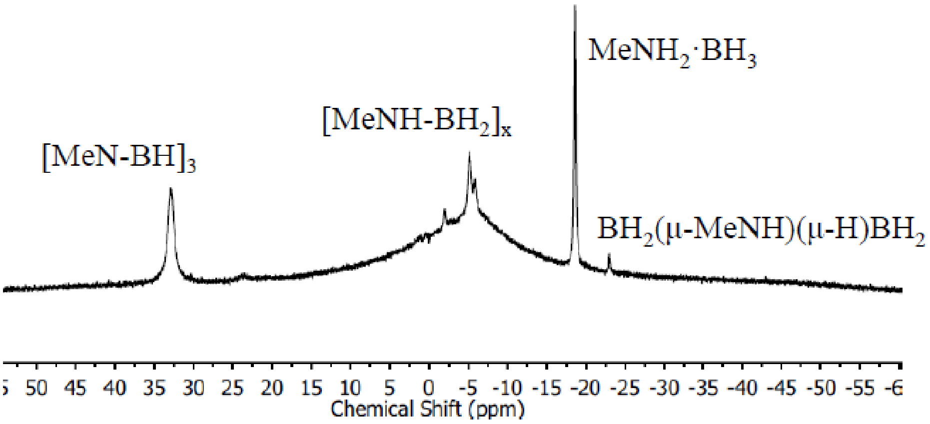

Figure S7(a): ^{11}B {^{1}H} NMR of reaction solution of [MeNH-BH$_2$]$_n$ after heating in toluene at 70 °C for 19 h.

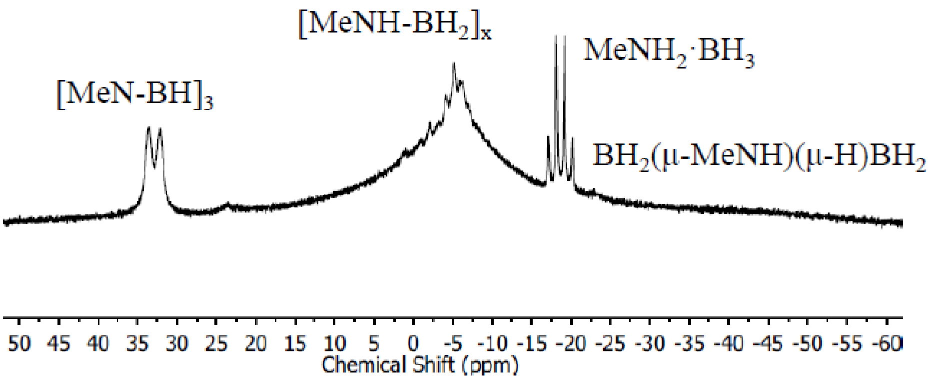

Figure S7(b): ^{11}B NMR of reaction solution of [MeNH-BH$_2$]$_n$ after heating in toluene at 70 °C for 19 h.

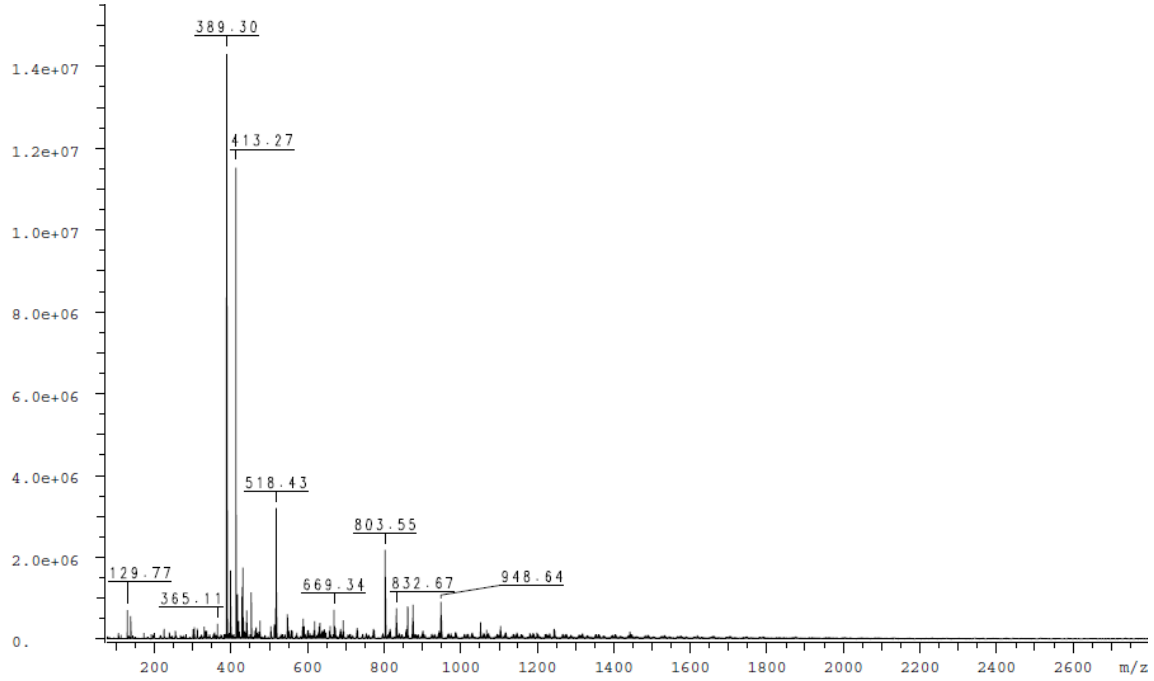

Figure S8(a): ESI-MS of reaction solution of $[MeNH\text{-}BH_2]_n$ after heating in toluene at 70 °C for 19 h.

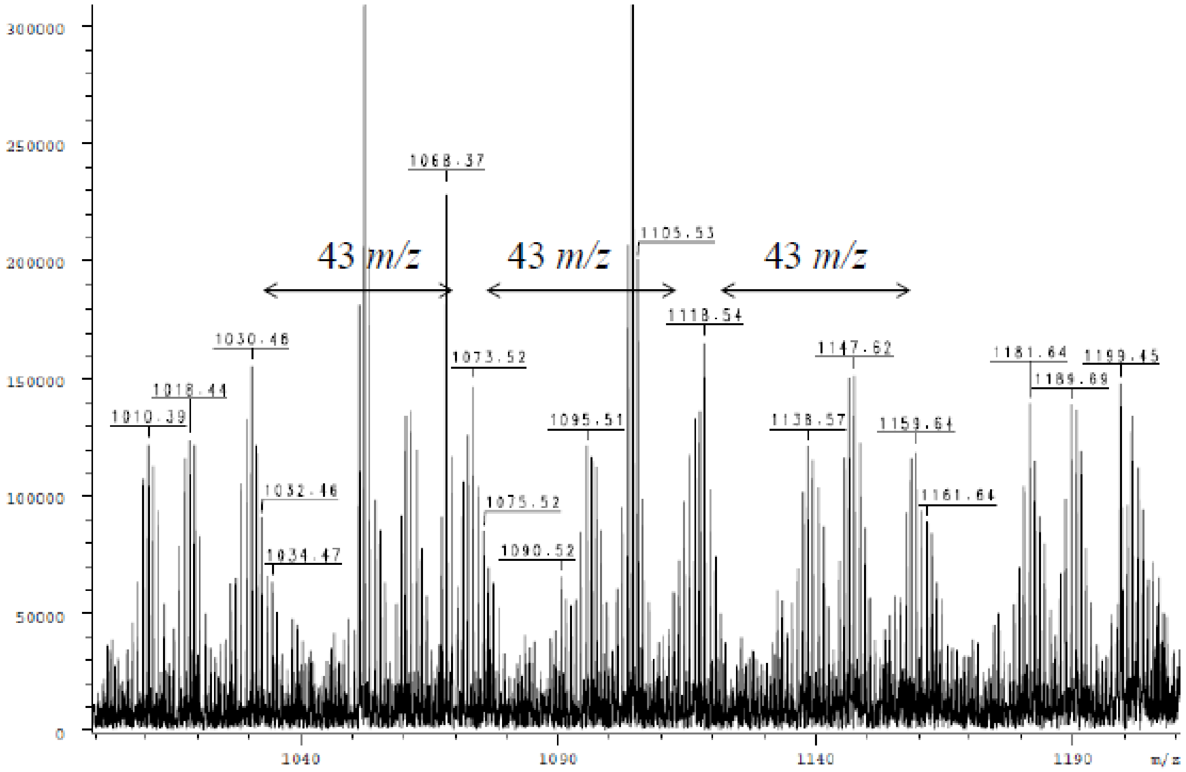

Figure S8(b): Enlarged view of a section of ESI-MS of reaction solution of $[MeNH\text{-}BH_2]_n$ after heating in toluene at 70 °C for 19 h.

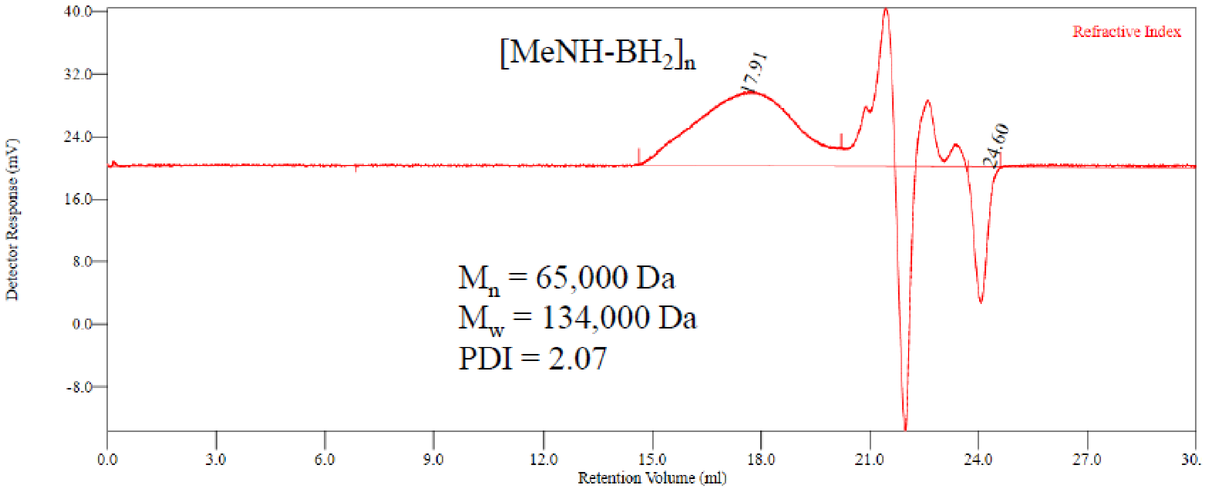

Figure S9: GPC trace of isolated $[MeNH\text{-}BH_2]_n$ after heating in toluene at 70 °C for 19 h. The various peaks at 21 – 24 min are a result of the sample injection.

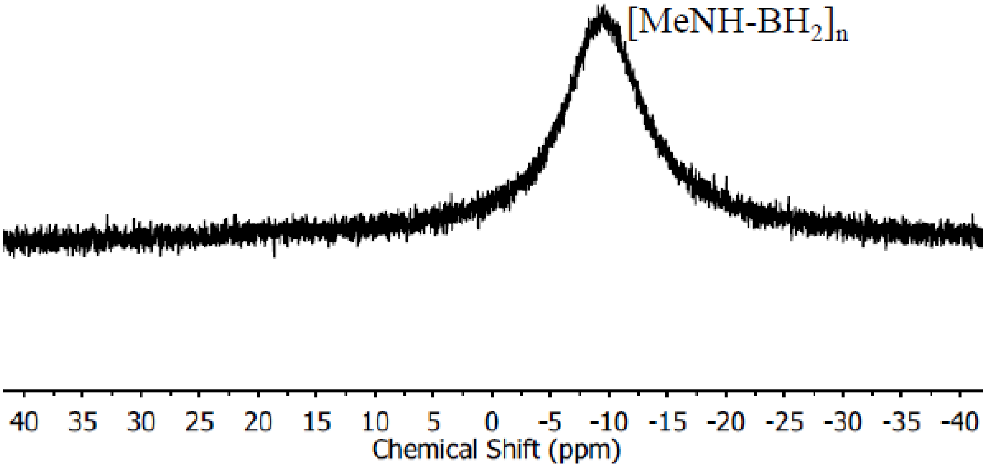

Figure S10: $^{11}B\{^1H\}$ NMR of reaction solution of $[MeNH\text{-}BH_2]_n$ and PCy_3 in toluene after heating at 50 °C for 22 h.

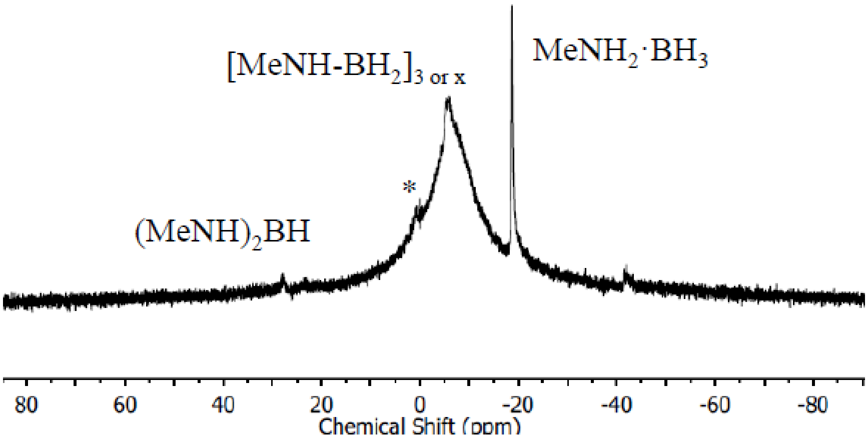

Figure S11(a): $^{11}B\ \{^1H\}$ NMR of the reaction solution of $[MeNH\text{-}BH_2]_n$ and P(*n*Bu)$_3$ in THF at 20 °C after 22 h. * Unknown product.

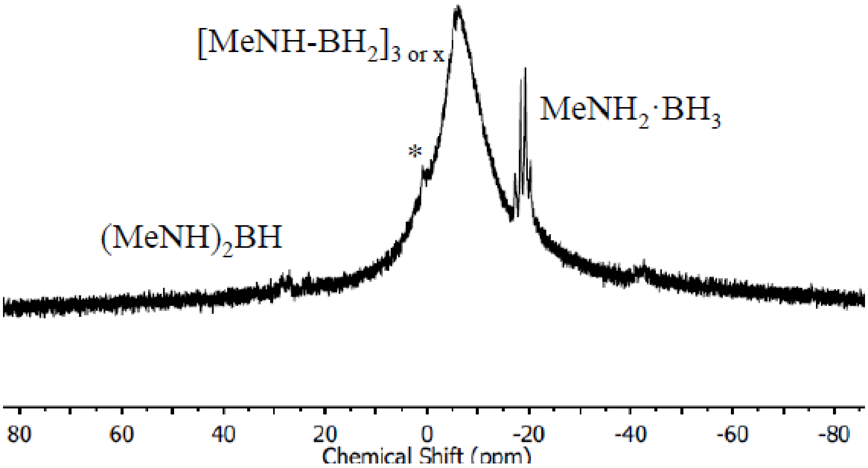

Figure S11(b): ^{11}B NMR of the reaction solution of $[MeNH\text{-}BH_2]_n$ and P(*n*Bu)$_3$ in THF at 20 °C after 22 h. * Unknown product.

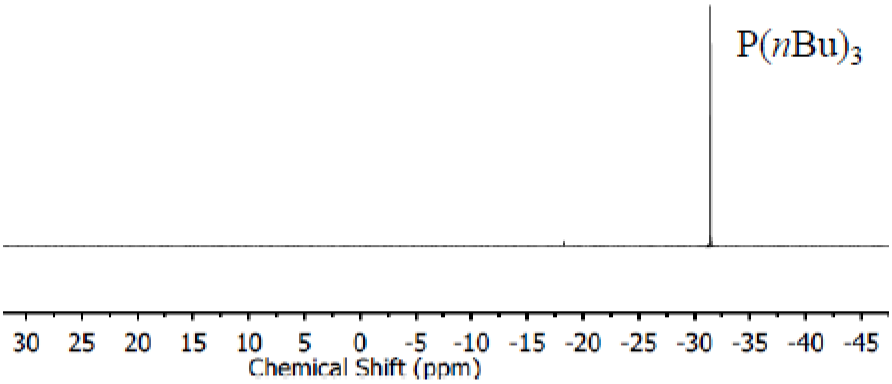

Figure S12: ^{31}P NMR of the reaction solution of $[MeNH\text{-}BH_2]_n$ and P(*n*Bu)$_3$ in THF at 20 °C after 22 h.

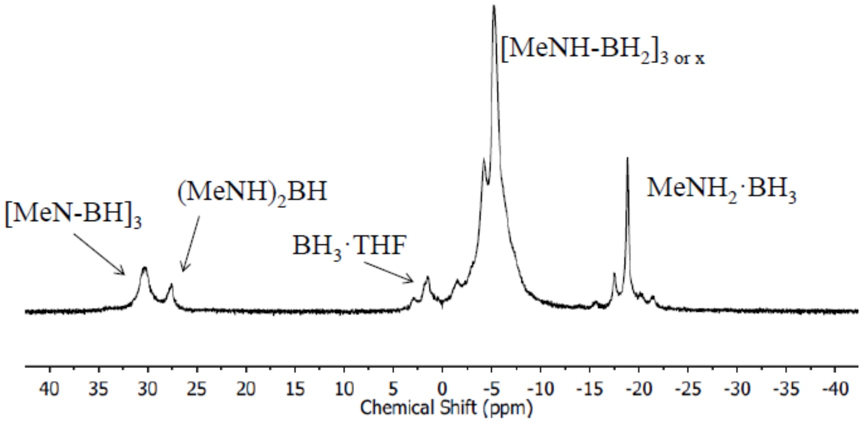

Figure S13(a): ^{11}B {^{1}H} NMR of the reaction solution of [MeNH-BH$_2$]$_n$ and DMAP in THF at 20 °C after 24 h.

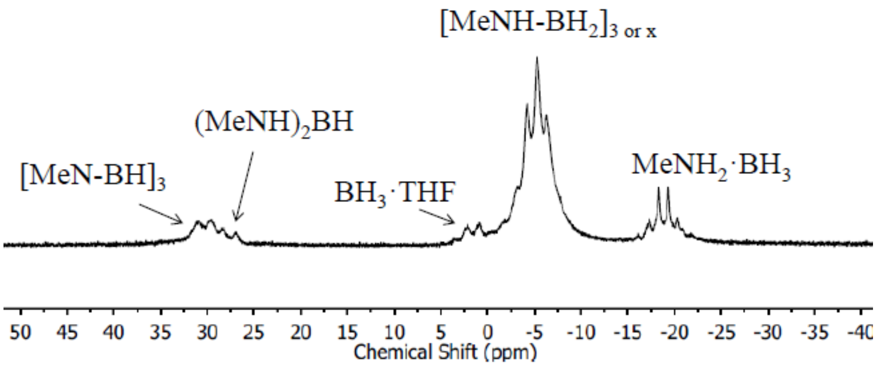

Figure S13(b): ^{11}B NMR of the reaction solution of [MeNH-BH$_2$]$_n$ and DMAP in THF at 20 °C after 24 h.

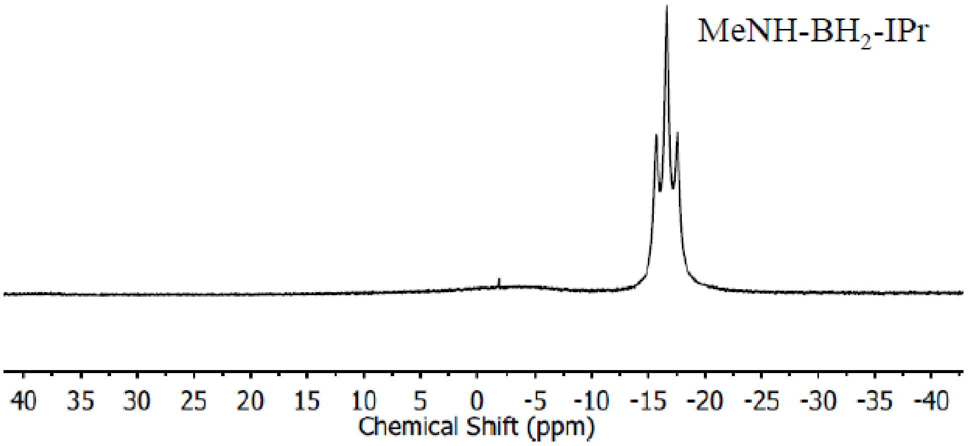

Figure S14a: ^{11}B NMR of reaction solution of [MeNH-BH$_2$]$_n$ and one equiv. IPr in THF at 20 °C after 10 min.

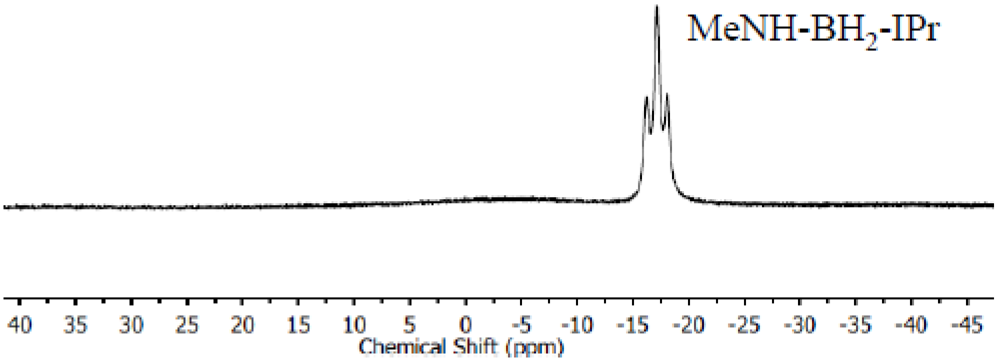

Figure S14b: ^{11}B NMR of reaction solution of [MeNH-BH$_2$]$_n$ and one equiv. IPr in THF at 20 °C after 1 h.

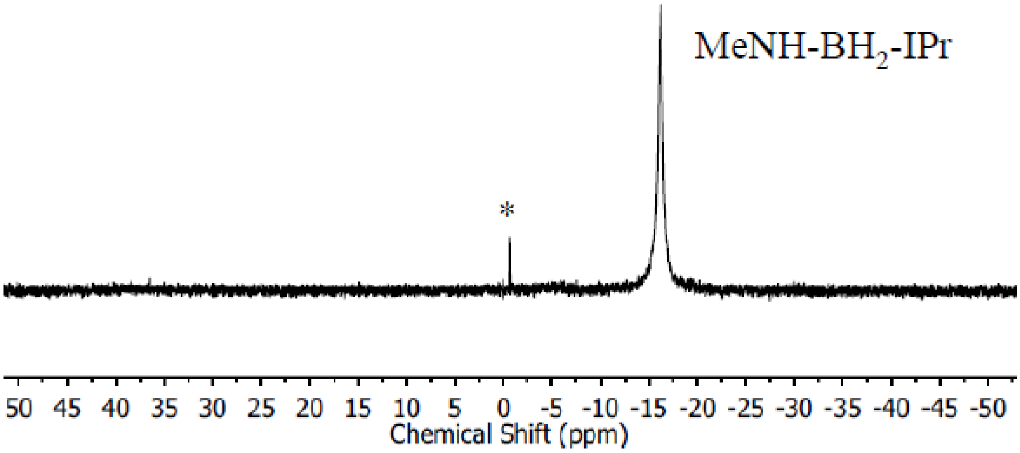

Figure S15(a): ^{11}B {^{1}H} NMR of isolated MeNH-BH$_2$-IPr in C_6D_6 at 20 °C. * Unknown product.

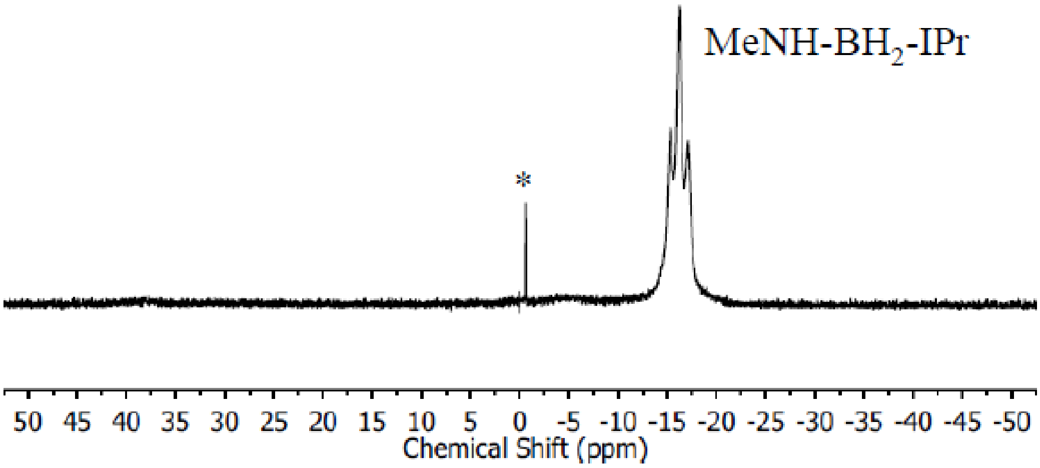

Figure S15(b): ^{11}B NMR of isolated MeNH-BH$_2$-IPr in C_6D_6 at 20 °C. * Unknown product.

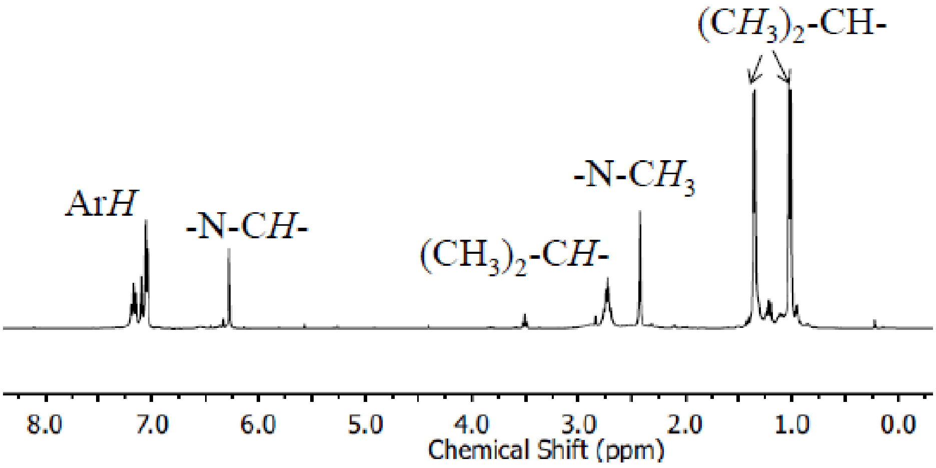

Figure S16: ^{1}H NMR of isolated MeNH-BH$_2$-IPr in C$_6$D$_6$ at 20 °C.

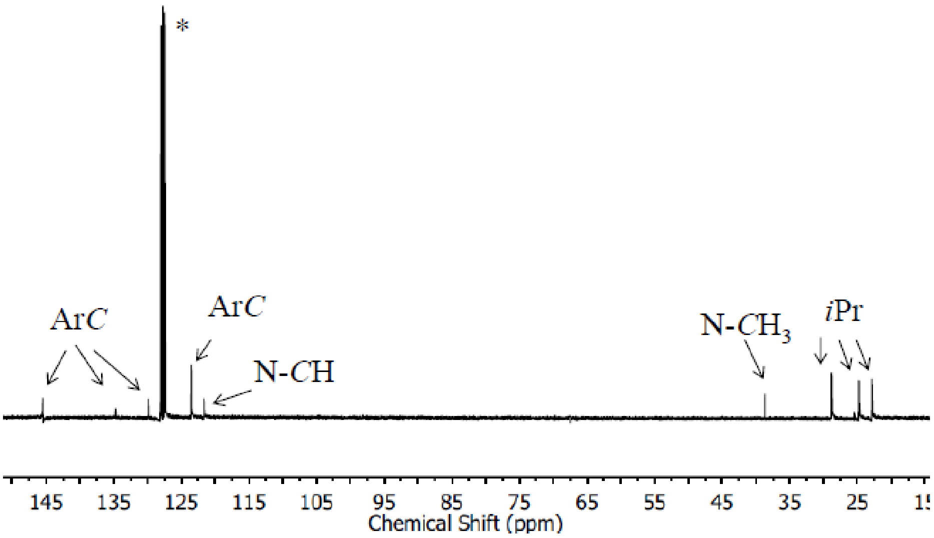

Figure S17: ^{13}C NMR of isolated MeNH-BH$_2$-IPr in C$_6$D$_6$ at 20 °C. * C$_6$D$_6$.

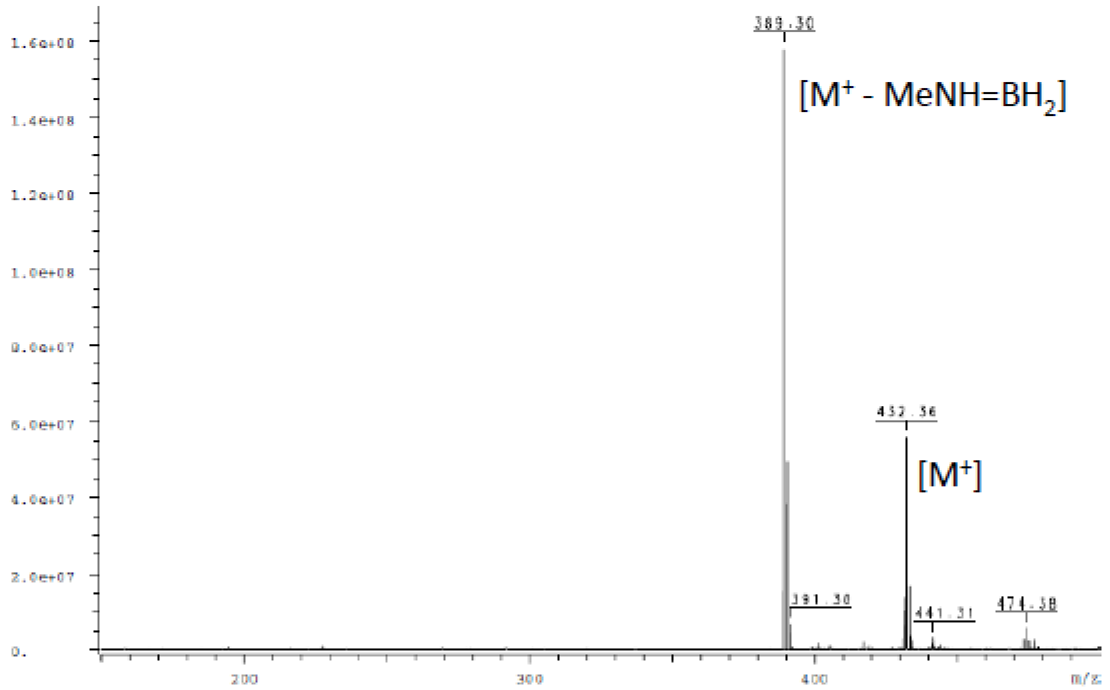

Figure S18: ESI-MS of reaction solution of $[MeNH\text{-}BH_2]_n$ and one equiv. IPr in THF at 20 °C ($[M^+]$ = $MeNH\text{-}BH_2\text{-}IPr$).

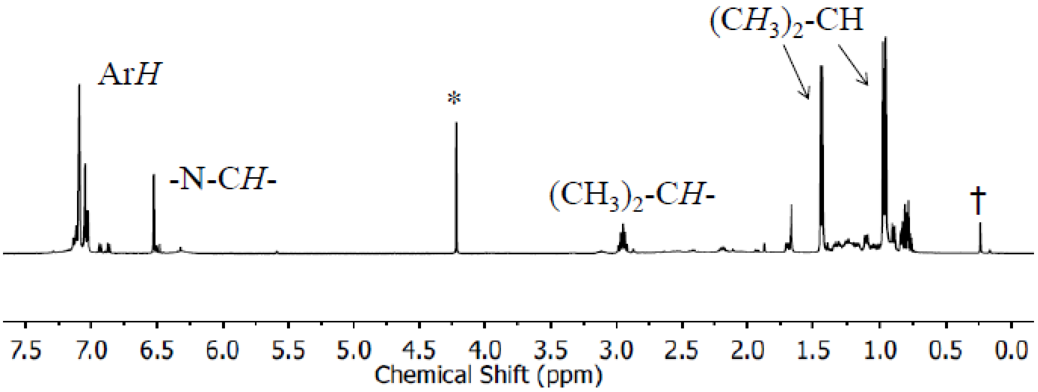

Figure S19: ^{1}H NMR of solid collected from attempted precipitation of $MeNH\text{-}BH_2\text{-}IPr$ using DCM and hexanes at 20 °C. * CH_2Cl_2, † Silicon grease.

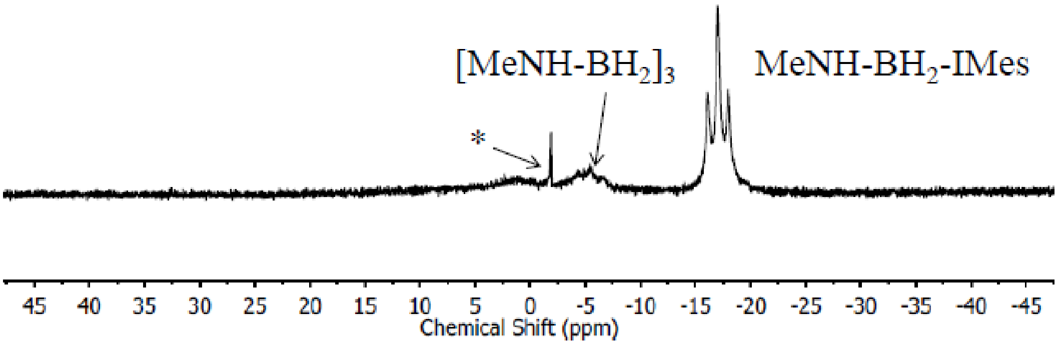

Figure S20: ^{11}B NMR of reaction solution of [MeNH-BH$_2$]$_n$ and one equiv. IMes in THF at 20 °C after 10 min. * Unknown product.

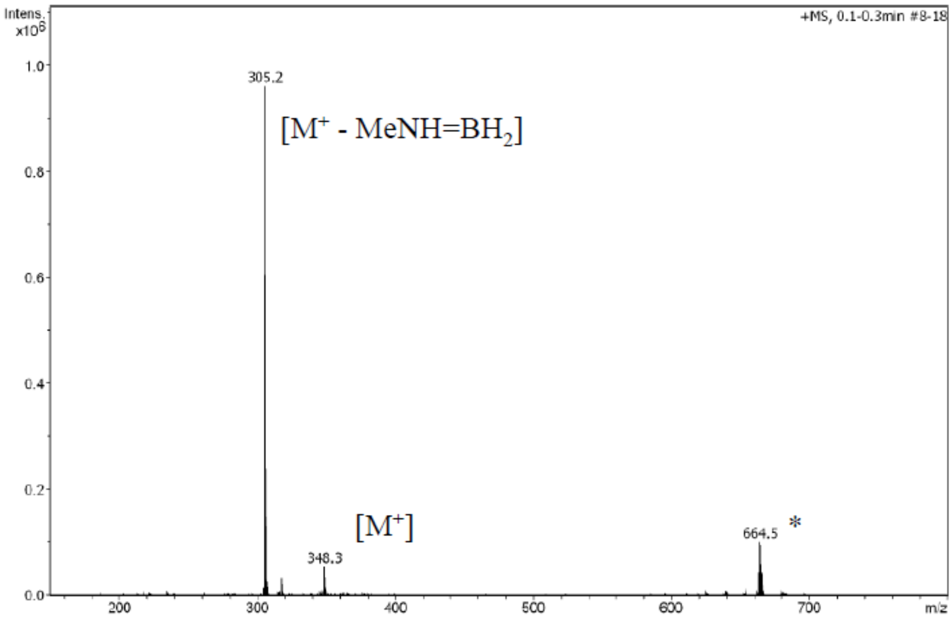

Figure S21: ESI-MS of reaction solution of [MeNH-BH$_2$]$_n$ and one equiv. IMes in THF at 20 °C ([M$^+$] = MeNH-BH$_2$-IMes). * This peak appears to be due to an impurity that is undetectable by NMR but may have the structure: MeN(BH$_2$(IMes))$_2$.

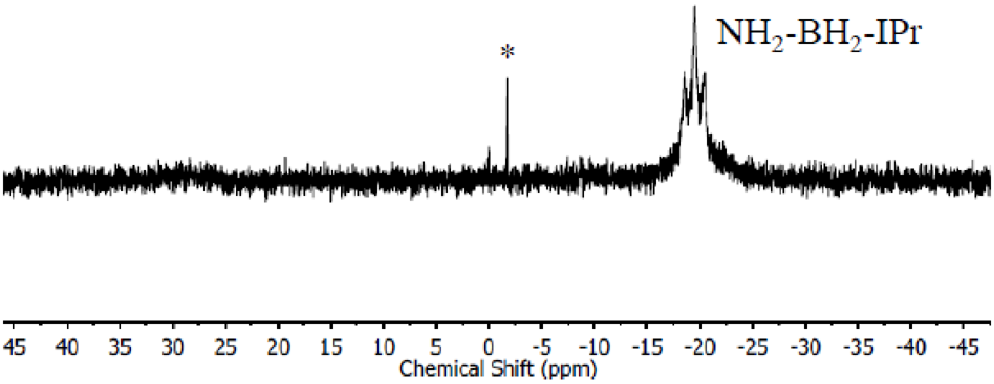

Figure S22: ^{11}B NMR of reaction solution of $[NH_2\text{-}BH_2]_n$ and one equiv. IPr in THF at 20 °C after 24 h. * Unknown product.

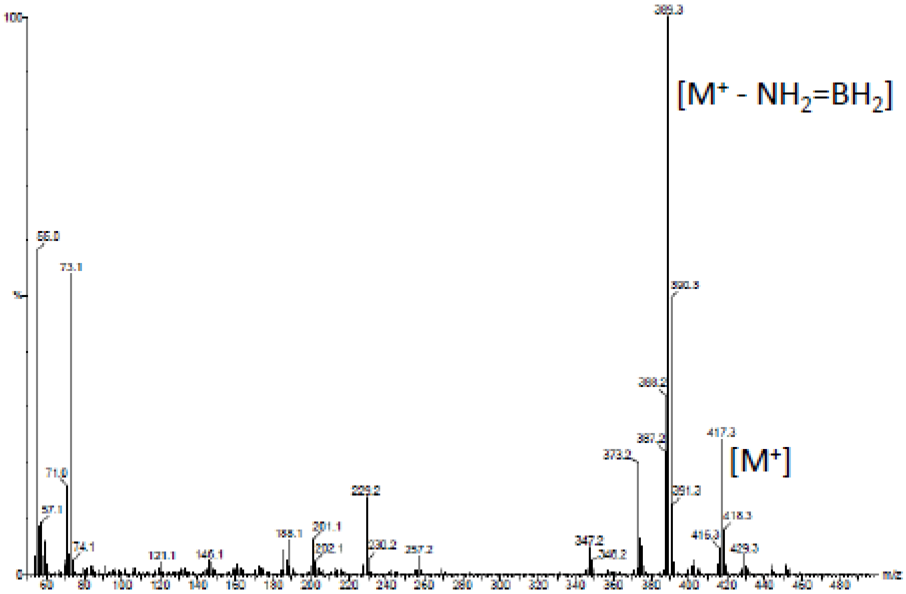

Figure S23: CI-MS of reaction solution of $[NH_2\text{-}BH_2]_n$ and one equiv. IPr in THF at 20 °C ($[M^+]$ = $NH_2\text{-}BH_2\text{-}IPr$).

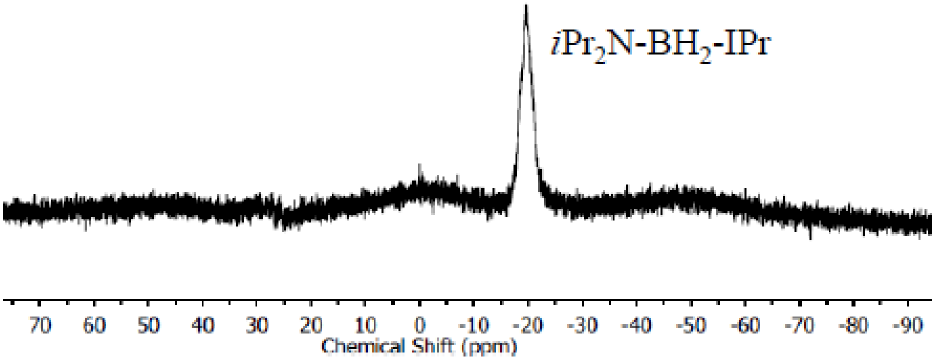

Figure S24: ^{11}B NMR of reaction of solution of *i*$Pr_2N{=}BH_2$ and one equiv. IPr in THF at 20 °C after 24 h.

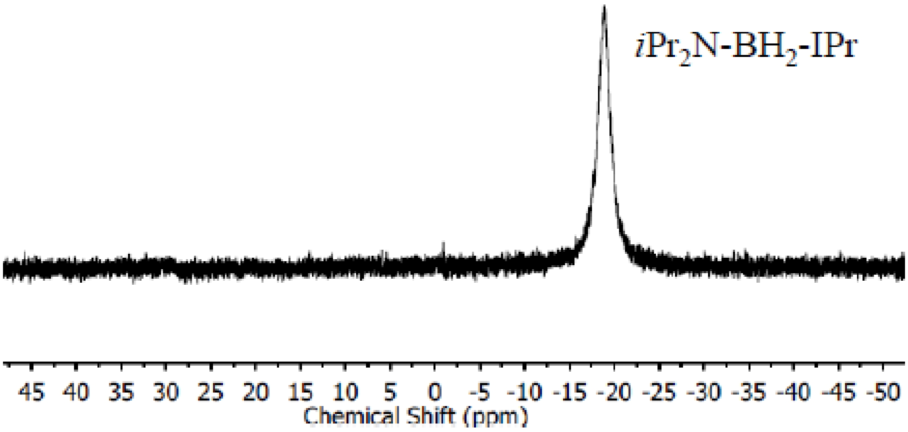

Figure S25(a): ^{11}B {^{1}H} NMR of isolated *i*Pr_2N-BH_2-IPr in C_6D_6 at 20 °C.

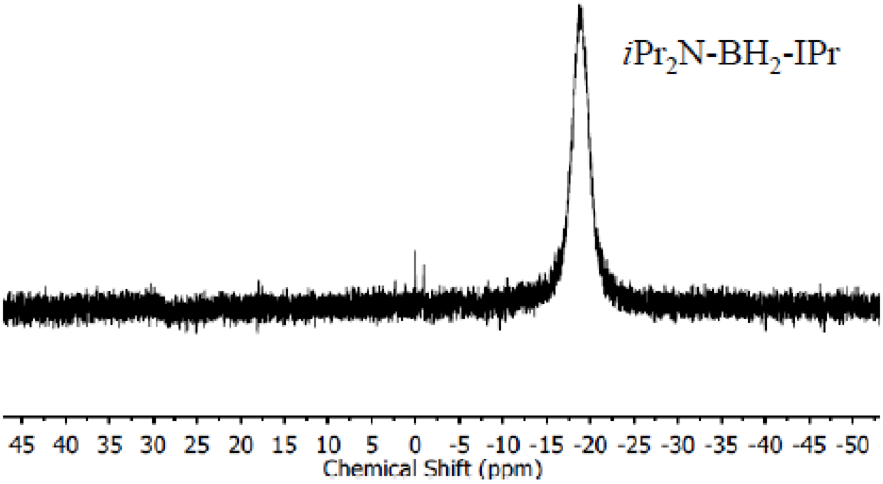

Figure S25(b): ^{11}B NMR of isolated *i*Pr_2N-BH_2-IPr in C_6D_6 at 20 °C.

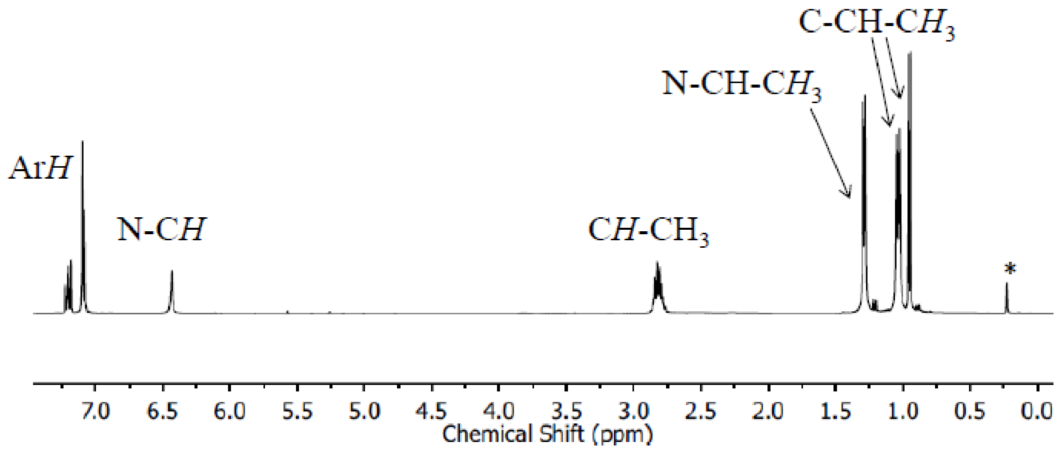

Figure S26: ^{1}H NMR of isolated *i*Pr$_2$N-BH$_2$-IPr in C_6D_6 at 20 °C. * Silicon grease.

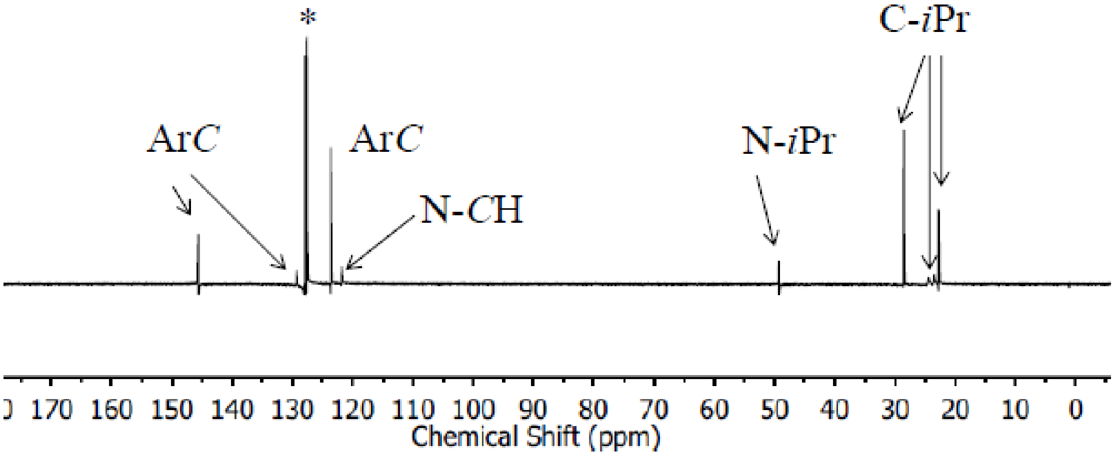

Figure S27: ^{13}C NMR of isolated *i*Pr$_2$N-BH$_2$-IPr in C_6D_6 at 20 °C. * C_6D_6.

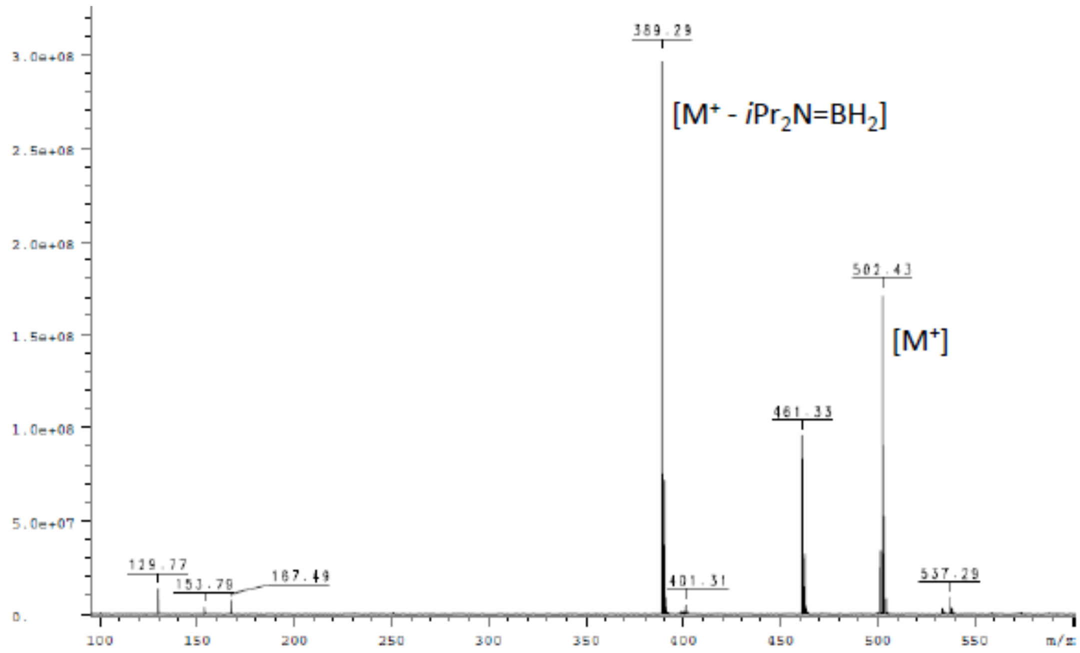

Figure S28: ESI-MS of reaction solution of $i\mathrm{Pr_2N{=}BH_2}$ and one equiv. IPr in THF at 20 °C ($[\mathrm{M}^+]$ = $i\mathrm{Pr_2N\text{-}BH_2\text{-}IPr}$).

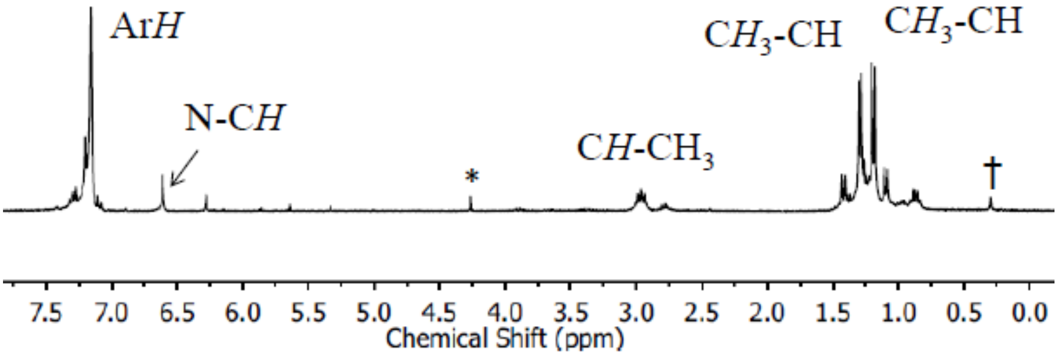

Figure S29: ^{1}H NMR of solid collected from attempted precipitation of $i\mathrm{Pr_2N\text{-}BH_2\text{-}IPr}$ using DCM and hexanes at 20 °C. * $\mathrm{CH_2Cl_2}$ *, † Silicon grease.

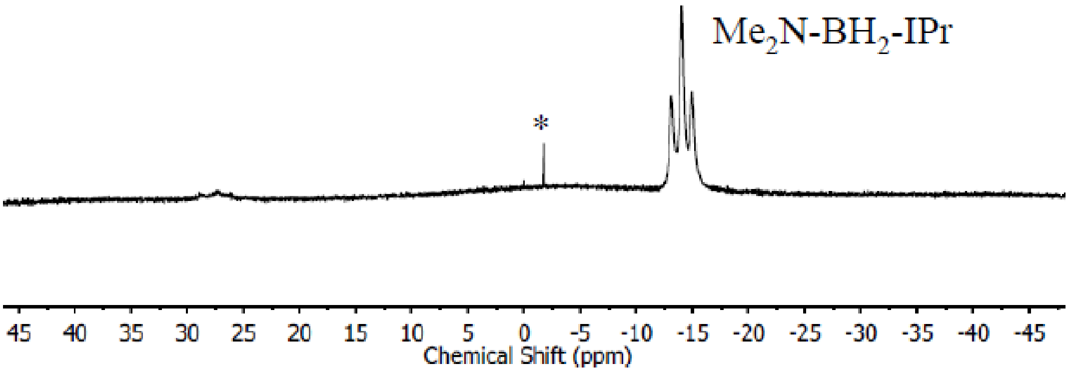

Figure S30: ^{11}B NMR of reaction solution of $[Me_2N-BH_2]_2$ and two equiv. IPr in THF at 60 °C after 24 h. * Unknown product.

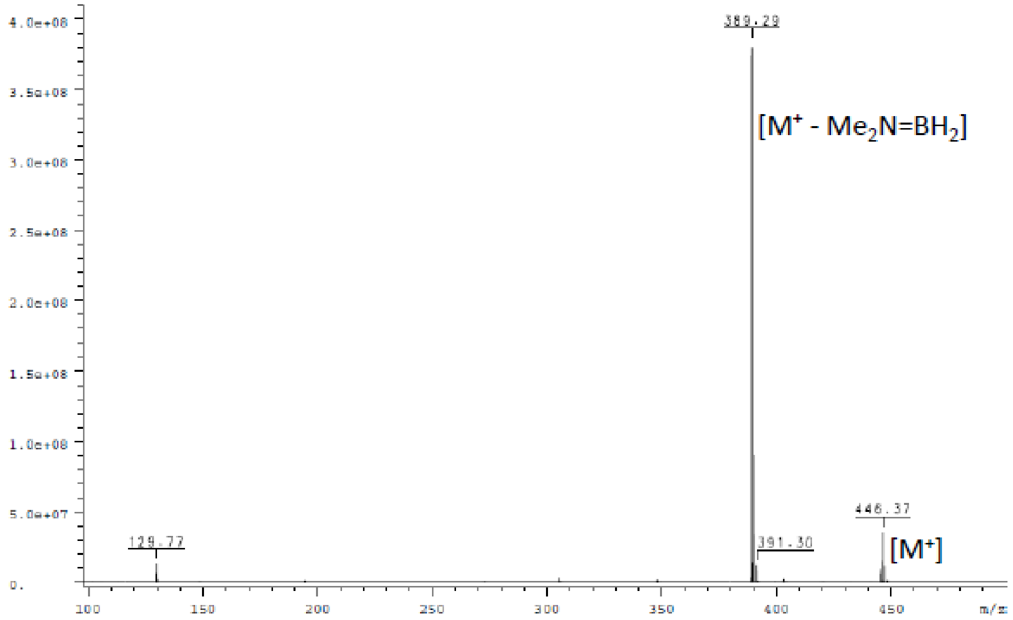

Figure S31: ESI-MS of reaction solution of $[Me_2N-BH_2]_2$ and two equiv. IPr in THF at 20 °C ($[M^+]$ = Me_2N-BH_2-IPr).

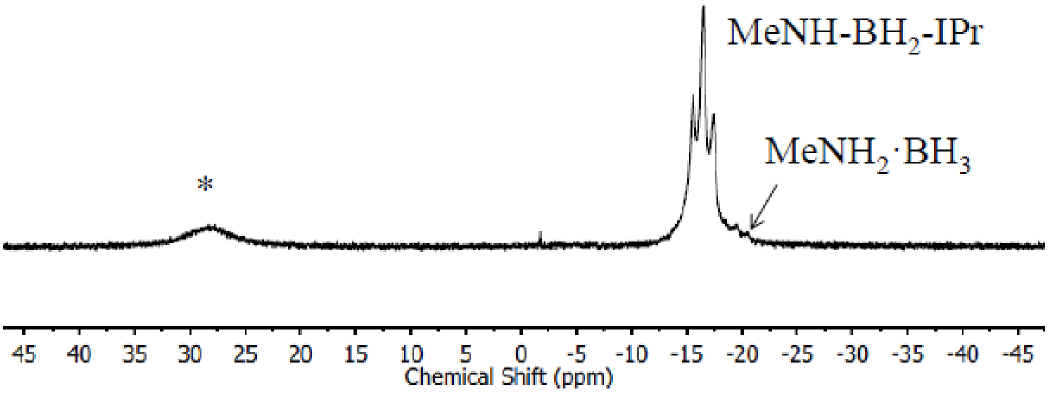

Figure S32: ^{11}B NMR of reaction solution of $MeNH_2·BH_3$ and two equiv. IPr in THF at 20 °C after 24 h. * Unknown product.

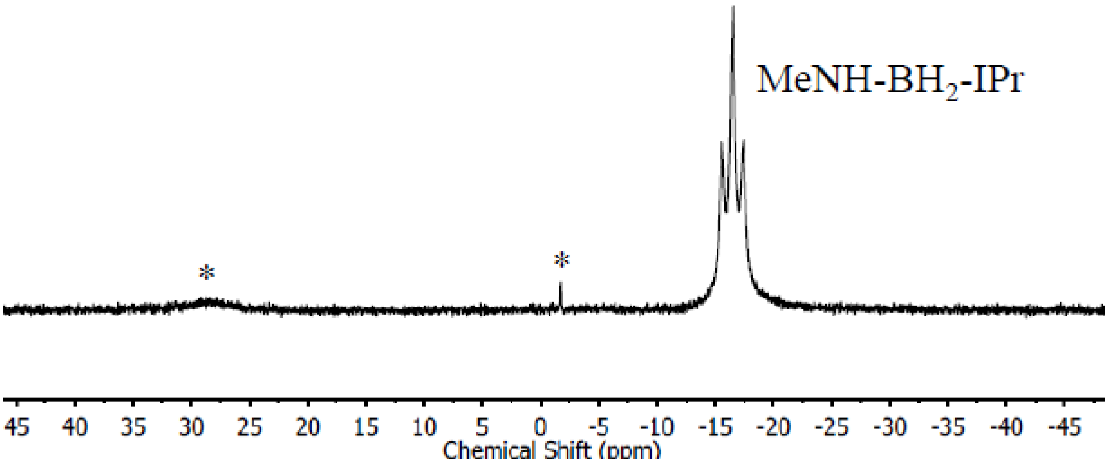

Figure S33: ^{11}B NMR of reaction solution of $MeNH_2·BH_3$ and 3 equiv. IPr in THF at 20 °C after 24 h. * Unknown products.

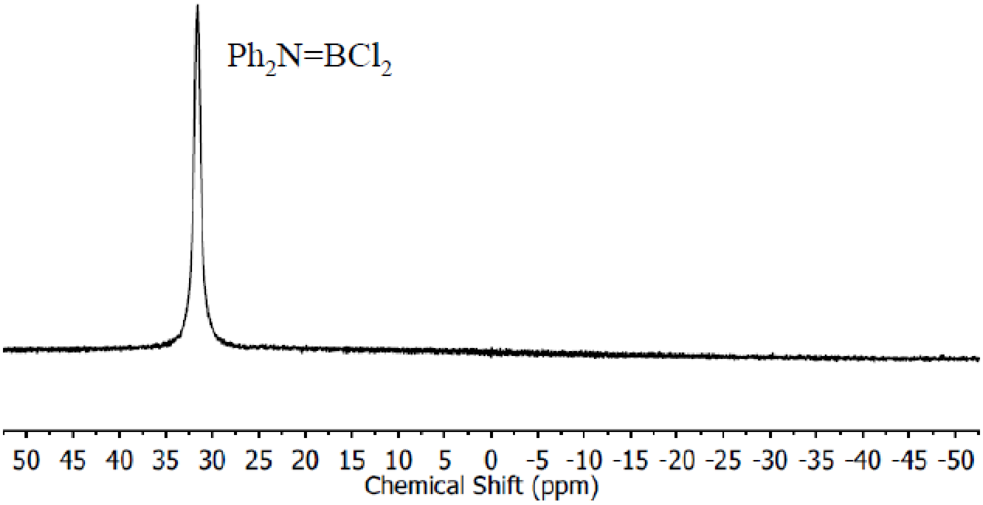

Figure S34: ^{11}B NMR of isolated $Ph_2N=BCl_2$ in C_6D_6 at 20 °C.

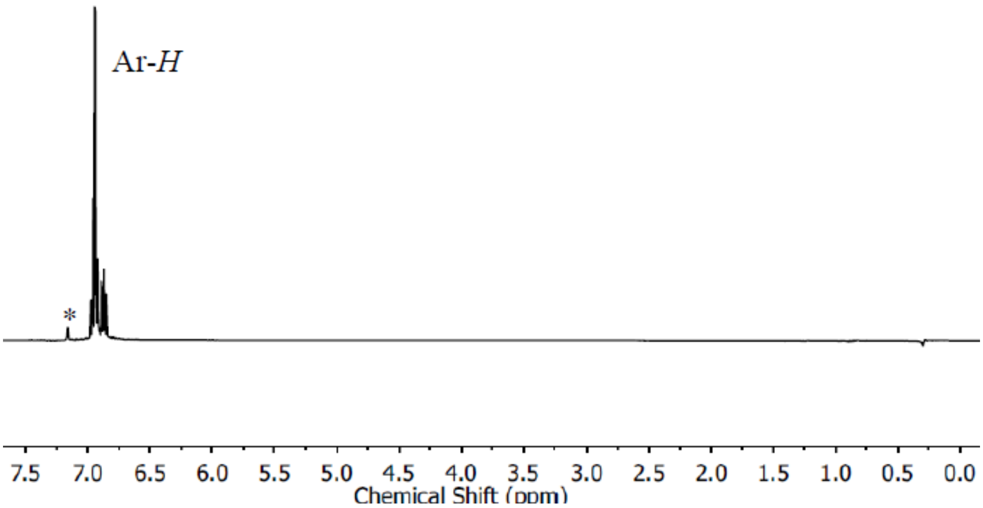

Figure S35: ^{1}H NMR of isolated $Ph_2N{=}BCl_2$ in C_6D_6 at 20 °C. * C_6D_6.

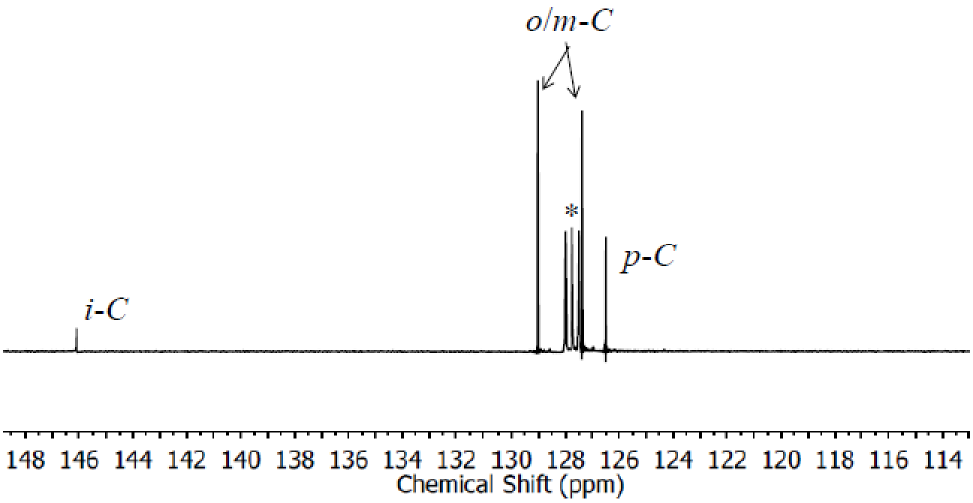

Figure S36: ^{13}C NMR of isolated $Ph_2N{=}BCl_2$ in C_6D_6 at 20 °C. * C_6D_6.

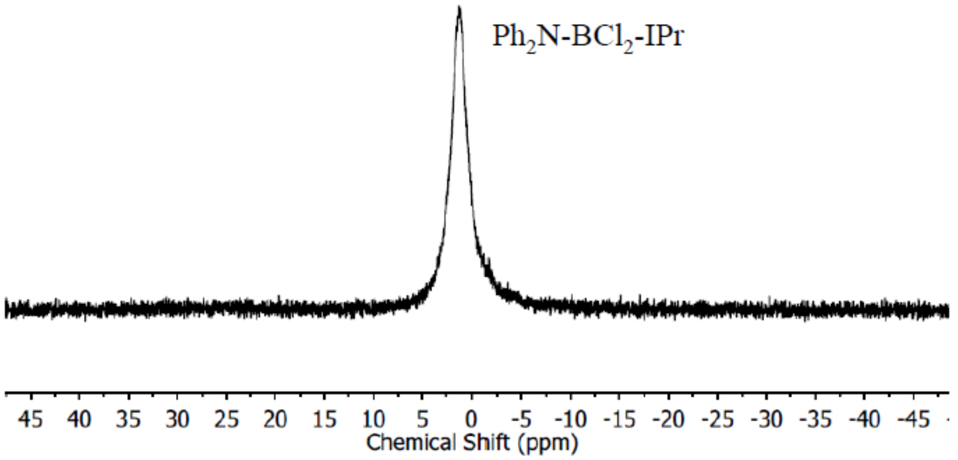

Figure S37: ^{11}B NMR of reaction solution of $Ph_2N=BCl_2$ and one equiv. of IPr in THF at 20 °C after 1 h.

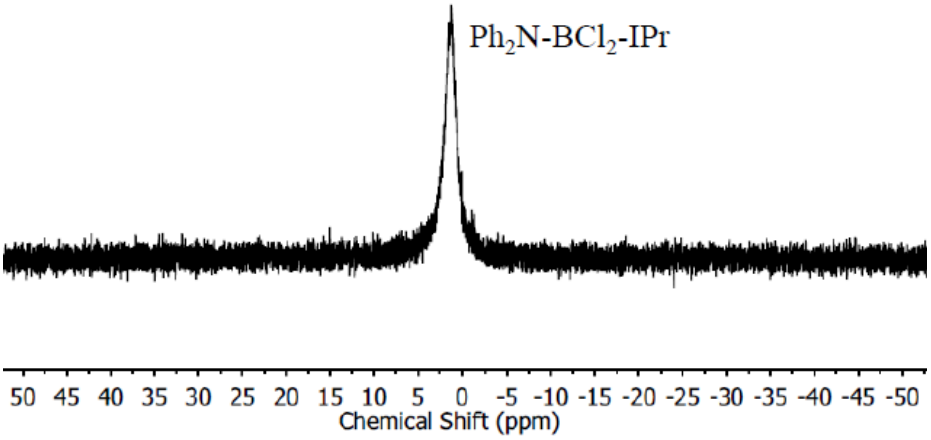

Figure S38: ^{11}B NMR of isolated **1** in C_6D_6 at 20 °C. The product was sparingly soluble in C_6D_6.

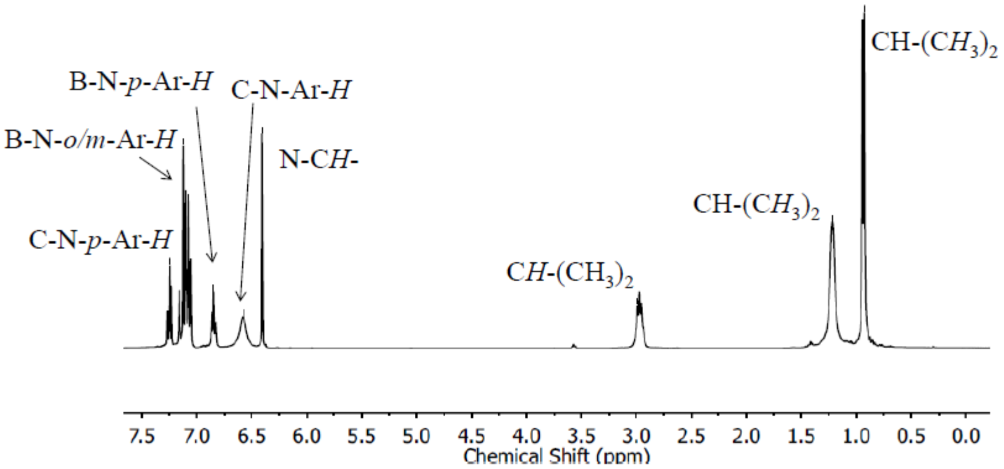

Figure S39: ^{1}H NMR of isolated **1** in C_6D_6 at 20 °C. The product was sparingly soluble in C_6D_6.

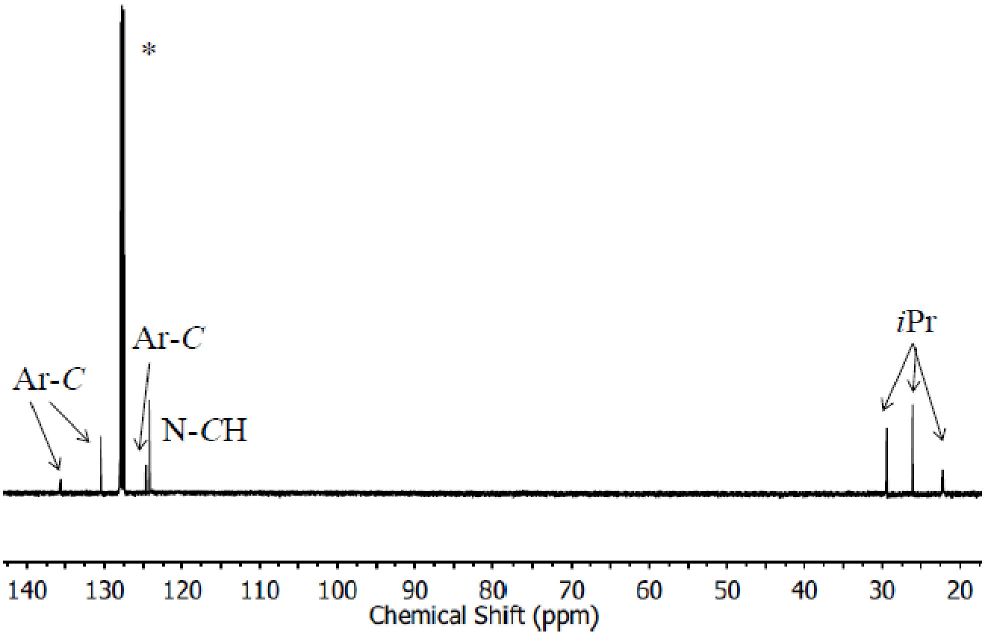

Figure S40: ^{13}C NMR of isolated **1** in C_6D_6 at 20 °C. The product was sparingly soluble in C_6D_6. * C_6D_6.

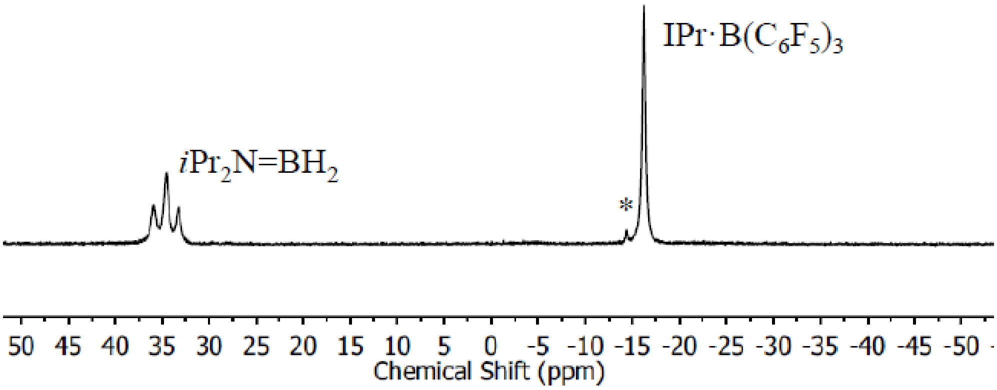

Figure 41: ^{11}B NMR of reaction solution of *i*Pr_2N-BH_2-IPr and one equiv. $B(C_6F_5)_3$ in toluene at 20 °C after 1h. * Unknown product.

Table S1: Reactions of aminoborane/amine-borane with IPr.

Substrate	**Equiv. of IPr**	**Duration (h)**	**(δ(^{11}B), THF) IPr-aminoborane adduct (ppm)**
$[MeNH\text{-}BH_2]_n$	1	1	-17.2 (t, $^1J_{BH}$ = 90 Hz)
$[NH_2\text{-}BH_2]_n$	1	24	-19.5 (t, $^1J_{BH}$ = 88 Hz)
iPr$_2$N=BH$_2$	1	2	-19.8 (br)
$[Me_2N\text{-}BH_2]_2$[a]	2	24	-14.1 (t, $^1J_{BH}$ = 89 Hz)
$MeNH_2{\cdot}BH_3$	2	8	-16.5 (t, $^1J_{BH}$ = 88 Hz)
$MeNH_2{\cdot}BH_3$	3	8	-16.5 (t, $^1J_{BH}$ = 90 Hz)

[a] Reaction performed at 60 °C.

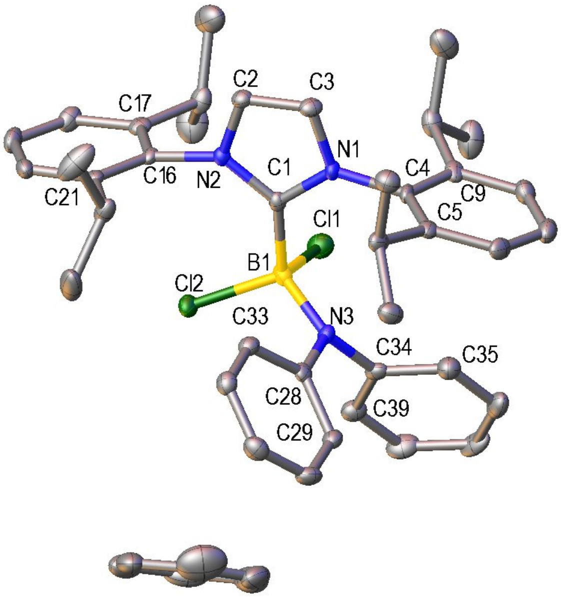

Figure S42: Molecular structure of compound **1** with one molecule of toluene of solvation determined by X-Ray diffraction with all non-H atoms as 50% thermal ellipsoids, and with all hydrogens removed for clarity.[3]

Table S2a: Crystal data and structure refinement for **1.**

Empirical formula	$C_{46}H_{54}BCl_2N_3$
Formula weight	730.63
Temperature/K	100(2)
Crystal system	orthorhombic
Space group	$P2_12_12_1$

a/Å	10.9067(10)
b/Å	19.265(2)
c/Å	19.688(2)
α/°	90.00
β/°	90.00
γ/°	90.00
Volume/Å^3	4136.8(7)
Z	4
ρ_{calc}mg/mm^3	1.173
m/mm^{-1}	0.192
F(000)	1560.0
Crystal size/mm^3	0.35 × 0.01 × 0.01
2Θ range for data collection	2.96 to 49.44°
Index ranges	$-12 \le h \le 12$, $-22 \le k \le 22$, $-23 \le l \le 23$
Reflections collected	99826
Independent reflections	7058[R(int) = 0.1072]
Data/restraints/parameters	7058/0/478
Goodness-of-fit on F^2	1.030
Final R indexes [I>=2σ (I)]	$R_1 = 0.0385$, $wR_2 = 0.0824$
Final R indexes [all data]	$R_1 = 0.0548$, $wR_2 = 0.0887$
Largest diff. peak/hole / e Å^{-3}	0.37/-0.42

Table S2b: Bond Lengths for **1.**

Atom	**Atom**	**Length/Å**	**Atom**	**Atom**	**Length/Å**
B1	C1	1.653(4)	C16	C17	1.396(3)

B1	Cl1	1.875(3)	C16	C21	1.398(3)
B1	Cl2	1.903(3)	C16	N2	1.459(3)
B1	N3	1.510(4)	C28	C29	1.406(4)
C1	N1	1.367(3)	C28	C33	1.406(4)
C1	N2	1.359(3)	C28	N3	1.404(3)
C2	C3	1.338(3)	C34	C35	1.389(4)
C2	N2	1.379(3)	C34	C39	1.381(4)
C3	N1	1.379(3)	C34	N3	1.438(3)
C4	C5	1.398(4)			
C4	C9	1.404(4)			
C4	N1	1.466(3)			

Table S2c: Bond Angles for **1.**

Atom	**Atom**	**Atom**	**Angle/°**	**Atom**	**Atom**	**Atom**	**Angle/°**
C1	B1	Cl1	105.76(17)	C33	C28	C29	116.7(2)
C1	B1	Cl2	108.18(17)	N3	C28	C29	122.0(2)
Cl1	B1	Cl2	105.52(13)	N3	C28	C33	121.3(2)
N3	B1	C1	115.4(2)	C35	C34	N3	120.1(2)
N3	B1	Cl1	110.48(17)	C39	C34	C35	119.1(3)
N3	B1	Cl2	110.89(18)	C39	C34	N3	120.8(2)
N1	C1	B1	126.0(2)	C1	N1	C3	110.7(2)
N2	C1	B1	129.5(2)	C1	N1	C4	128.86(19)
N2	C1	N1	104.4(2)	C3	N1	C4	120.41(19)
C3	C2	N2	107.5(2)	C1	N2	C2	110.59(18)
C2	C3	N1	106.9(2)	C1	N2	C16	131.6(2)

C5	C4	C9	123.7(2)	C2	N2	C16	117.6(2)
C5	C4	N1	118.0(2)	C28	N3	B1	121.56(19)
C9	C4	N1	117.8(2)	C28	N3	C34	115.1(2)
C4	C5	C6	116.3(2)	C34	N3	B1	119.1(2)
C17	C16	C21	123.4(2)				
C17	C16	N2	117.9(2)				
C21	C16	N2	118.2(2)				

References:

1. A. Staubitz, A. P. Soto and I. Manners, *Angew. Chem. Int. Ed.*, 2008, **47**, 6212; A. Staubitz, M. E. Sloan, A. P. M. Robertson, A. Friedrich, S. Schneider, P. J. Gates, J. S. auf der Günne and I. Manners, J. Am. Chem. Soc., 2010, 132, 13332.

2. C. A. Jaska, K. Temple, A. J. Lough and I. Manners, *J. Am. Chem. Soc.*, 2003, **125**, 9424.

3. X-Ray structure figures generated with Olex2 software; O. V. Dolomanov, L. J. Bourhis, R. J. Gildea, J. A. K. Howard and H. Puschmann, OLEX2: a complete structure solution, refinement and analysis program. *J. Appl. Cryst.,* 2009, **42**, 339.